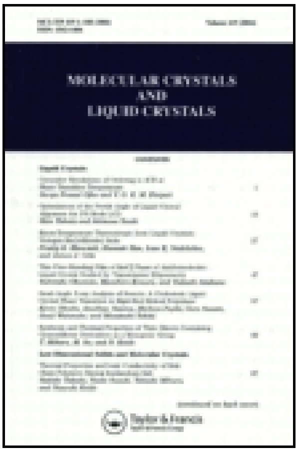

Molecular Crystals and Liquid Crystals
Publication details, including instructions for authors and subscription information:
http://www.tandfonline.com/loi/gmcl16

The Structure of Open Merocyanine Forms of Photochromic Indoline Spiropyrans and the Mechanism of Their Structural Conversions

S. M. Aldoshin [a] & L. O. Atovmyan [a]

[a] Institute of Chemical Physics of the USSR Academy of Sciences, Chernogolovka, Moscow Region, 142432, USSR

To cite this article: S. M. Aldoshin & L. O. Atovmyan (1987): The Structure of Open Merocyanine Forms of Photochromic Indoline Spiropyrans and the Mechanism of Their Structural Conversions, Molecular Crystals and Liquid Crystals, 149:1, 251-290

To link to this article: http://dx.doi.org/10.1080/00268948708082985

Mol. Cryst. Liq. Cryst., 1987, Vol. 149, pp. 251–290
Photocopying permitted by license only

Printed in the United States of America

The Structure of Open Merocyanine Forms of Photochromic Indoline Spiropyrans and the Mechanism of Their Structural Conversions

S. M. ALDOSHIN and L. O. ATOVMYAN

Institute of Chemical Physics of the USSR Academy of Sciences, Chernogolovka, Moscow Region, 142432, USSR

(*Received August 19, 1986; in final form April 2, 1987*)

The results of the structure study of open merocyanine forms of indoline spiropyrans are reported. Structural factors stabilizing spiropyrans in the open state are discussed. The molecular and crystal structures of these compounds are discussed in detail as well as the intermolecular interaction energy in their crystals and the thermal stability of various isomers. From the point of view of the data obtained the most probable mechanism of spiropyrans photoconversions is considered.

I. INTRODUCTION

Photochromic materials are known to be employed in various branches of science and technology.[1] Spiropyrans (SP) of the indoline series are one of the most promising photochromic systems.[2] However, despite the intensive studies of these compounds, the mechanism of SP photochromic conversions and the relation between their structure and photochemical properties have not been quite elucidated. Earlier,[3,4] based on the analysis of SP structure and photochromic properties, we have shown the SP photochemical properties to be mainly explained by the fact that already in the ground state the C_{spiro}—O bond ruptured upon photoexcitation is extended and weakened due to specific orbital interactions which increase in the excited state to result in the heterolytic dissociation of the bond. The structural factors affecting the above interactions, the length of the C_{spiro}—O bond and the quantum yield of the bond rupture have been found out.

Another important characteristic of the SP photochromic systems is the lifetime of the open merocyanate (MC) SP forms, hence, it is necessary to investigate in detail the MC forms structure and to find out the structural factors stabilizing SP in the open state.

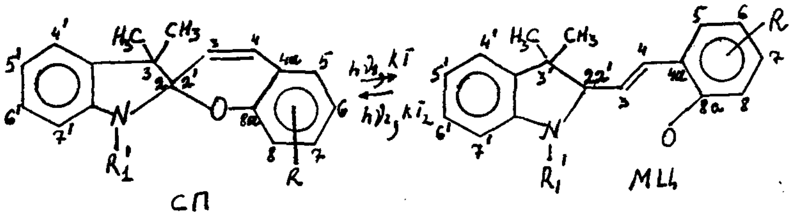

I: $R_1' = CH_3$; $R_6 = NO_2$; $R_8 = Br$
II: $R_1' = C_5H_{11}$; $R_6 = NO_2$; $R_8 = Br$; $R_6 = NO_2$; $R_8 = NO_2$;
III, IV: $R_1' = p—CH_3—C_5H_{10}$;
V: $R_1' = H$; $R_6 = NO_2$; $R_8 = NO_2$.

Our paper summarizes the results of the X-ray structure investigation of MC crystals I–V and makes a detailed analysis of crystal and molecular structures of their compounds, the energy of intermolecular interactions in crystals, thermodynamic and kinetic stability of the discovered isomers. On these grounds the most probable structural mechanism of SP phototransformations is considered.

II. EXPERIMENTAL

The major crystallographic data for the investigated MC I–V are listed in Table I. An experimental set of the reflections with $I \geq 2\sigma(I)$ from the MC crystals I–V was obtained on a DAR-UM automatic diffractometer with CuKα-irradiation, graphite monochromator using the $\omega - \omega/2\omega$ technique for each layer. No absorption correction was applied. The structures were solved by the direct methods and the heavy atom technique (MC I and II) by a complex of the "Roentgen-75" programs[5] and refined by a full-matrix least-squares technique in anisotropic (non-hydrogen atoms) approximation. Only the positional parameters were refined for hydrogen atoms, and the latter were assigned the isotropic thermal parameters $B_{iso} = B_{com} + I$. Due to strong thermal vibrations of C_{12}' and C_{13}' atoms in the MC II structure their hydrogen atoms failed to be localized. The phenolate oxygen O_1 atom was discovered on E-syntheses in the structures of MC IV and III simultaneously both in cis- and trans-sites relative to the

TABLE I

The main crystallographic data on MC I–V

	MC I	MC II	MC III	MC IV	MC V
Formula	$C_{19}H_{17}BrN_2O_3 \cdot H_2O$	$C_{23}H_{25}BrN_2O_3$	$C_{26}H_{23}N_3O_5 \cdot 1/2H_2O$	$C_{26}H_{23}N_3O_5 \cdot 1/2H_2O \cdot 1/4H_2O$	$C_{19}H_{17}N_3O_5$
a (Å)	8.628(3)	10.996(6)	14.120(5)	18.601(4)	8.924
b	7.255(3)	8.301(3)	16.329(9)	37.835(16)	13.955
c	29.063(16)	23.641(3)	20.195(8)	7.008(2)	14.126
α(°)	90	90	90	90	90
β	90	90	90	90	90
γ	101°46′(3)′	83°36′(3)′	84°40′(3)′	90	81°44′(3)′
Space group	$P2_1/b$	$P2_1/n$	B2/b	Aba2	P21/n
V (Å^3)	1783(3)	2144(3)	4636(3)	4932(3)	1741(3)
M	419.28	457.37	466.49	470.99	367.36
Z	4	4	8	8	4
d_{calc} (g/cm^3)	1.572(4)	1.425(3)	1.344(3)	1.276(3)	1.410(3)
The number of independent non-zero reflections	1222	1622	1523	1053	892
Type of reflection	hK0–hK28	hK0–hK22	hK0–hK19	hK0–hK7	hK0–hK14
θ region (°)	$5.2° \leq \theta \leq 50.8°$	$5.4° \leq \theta \leq 50.4°$	$3.8 \leq \theta \leq 50.3°$	$2.3° \leq \theta \leq 57.7°$	$4.5° \leq \theta \leq 56.4°$
Crystal size (mm)	0.2 × 0.15 × 0.05	0.17 × 0.25 × 0.20	0.20 × 0.25 × 0.30	0.15 × 0.15 × 0.55	0.23 × 0.23 × 0.05
R	0.045	0.049	0.061	0.074	0.046

$T_{anis} = \exp - (b_{11}h^2 + b_{22}K^2 + b_{33}l^2 + b_{12}hK + b_{13}hl + b_{23}Kl)$.

vinyl $C_3{=}C_4$ group. The heights of the electron density peaks corresponding to the O_1 and O'_1 atoms in these sites have appeared to be twice as low as for the other oxygen atoms. A simultaneous refinement of the isotropic thermal factors of the O_1 and O'_1 oxygen atoms and the population of their site has shown the O_1 and O'_1 atoms to occupy ~50% of their site. This points at the statistic disorder of the whole of the phenolate fragment which is symmetrical with respect to the $C_4{-}C_{4a}$ bond and the existence in the crystals of trans–cis and trans–trans isomers in nearly equal concentrations. The MC IV crystal structure has an inversion pseudocentre between the molecules connected by a rotational symmetry axis C_2 which complicated considerably the structure refinement and accounted for heavy errors in the atom coordinates determination and high value of R-factor. Besides, the N'_1-p-tolyl substituent makes strong thermal vibrations about the $N'_1{-}C'_{10}$ bond, which interferes with atom refinement. As a result, we have failed to localize the hydrogen atoms in the p-tolyl fragment of the molecule. The hydrogen atoms could not be localized also in the MC III and IV structures of the statistically disordered water molecules. The pictures of the molecules with probability ellipsoids of atomic thermal vibrations were performed with the "Ellids" program.[6] The MC I and II atomic coordinates were reported by us earlier elsewhere,[7,8] those of the MC III–IV are listed in Tables II–IV. The main MC I–V bond lengths and valence angles are given in Figures 1, 3–6. Quantum-chemical calculations of the MC electronic structure are performed by the "Viking" program using the CNDO/2 method.[9] The molecule geometry obtained from the X-ray analysis was used for the calculations. Figure 7 visualizes the charge distribution on the atoms of the investigated MC I, II, V molecules. The evaluation of the intermolecular interaction energy (IMIE) in crystals was made in the framework of the atom–atom approximations using the "6-exp" potential φ_{ij} and taking into account the electrostatic component φ_{ij}.[10]

$$u = \frac{1}{2}\Sigma(\mathrm{u}_{ij} + \psi_{ij})$$

$$\varphi_{ij} = -A_{mn}r_{ij}^{-6} + B_{mn}\exp(-\alpha_{mn}r_{ij})$$

$$\psi_{ij} = \Sigma q_i q_j / r_{ij}$$

where A, B and α are the empirical parameters, r_{ij} is the interatomic

TABLE II

Coordinates of non-hydrogen (x 10^4) and hydrogen (x 10^3) atoms in the MC III molecule

Atoms	X	Y	Z	Atoms	X	Y	Z
O_1	4100(6)	3483(4)	3222(4)	C_4^a	3773(3)	3104(3)	2128(2)
$O_{1'}$	3538(6)	2616(4)	1051(4)	C_5	3632(4)	2463(3)	1647(3)
O_2	3896(4)	2428(3)	4114(2)	C_6	3585(4)	1669(3)	1912(3)
O_3	3988(1)	1183(3)	3859(3)	C_7	3676(4)	1495(3)	2573(3)
O_4	3322(6)	1125(3)	887(3)	C_8	3812(4)	2115(3)	3008(3)
O_5	3388(5)	314(3)	1688(3)	C_{8a}	3866(4)	2938(3)	2812(3)
$N_{1'}$	3942(3)	6101(2)	2238(2)		4880(6)	2943(4)	358(4)
N_2	3913(4)	1904(4)	3706(3)	$H_{4'}$	312(4)	706(3)	25(2)
N_3	3424(4)	997(3)	1473(3)	$H_{6'}$	364(3)	886(3)	166(2)
$C_{22'}$	3804(3)	5417(3)	1888(2)	$H_{7'}$	394(4)	775(3)	256(2)
$C_{3'}$	3557(3)	5652(3)	1182(2)	$H_{8.1'}$	493(4)	544(3)	90(2)
$C_{4'}$	3346(4)	7161(3)	739(3)	$H_{8.2'}$	424(4)	555(3)	34(2)
$C_{4a'}$	3533(4)	6579(3)	1221(3)	$H_{8.3'}$	436(4)	464(3)	62(2)
$C_{5'}$	3381(4)	8003(3)	895(3)	$H_{9.1'}$	213(4)	559(3)	132(2)
$C_{6'}$	3602(4)	8209(3)	1550(3)	$H_{9.2'}$	255(4)	474(3)	95(2)
$C_{7'}$	3803(4)	7628(3)	2040(3)	$H_{9.3'}$	247(4)	558(3)	42(2)
$C_{7a'}$	3757(3)	6813(3)	1848(2)	$H_{11'}$	308(3)	666(3)	334(2)
$C_{8'}$	4361(4)	5313(4)	714(3)	$H_{12'}$	384(4)	682(3)	447(2)
$C_{9'}$	2593(4)	5393(3)	945(3)	$H_{14'}$	639(4)	556(3)	369(2)
$C_{10'}$	4338(3)	6108(2)	2899(2)	$H_{15'}$	558(3)	549(3)	256(2)
$C_{11'}$	3837(4)	6476(3)	3409(2)	$H_{16.1'}$	584(3)	560(3)	503(2)
$C_{12'}$	4246(4)	6474(3)	4030(3)	$H_{16.2'}$	529(4)	633(3)	534(2)
$C_{13'}$	5189(5)	6121(4)	4125(3)	$H_{16.3'}$	622(4)	630(3)	470(2)
$C_{14'}$	5670(4)	5759(3)	3593(3)	$H_{17.1'}$	266(4)	882(3)	36(2)
$C_{15'}$	5269(4)	5750(3)	2989(2)	$H_{17.2'}$	283(3)	848(3)	5(2)
$C_{16'}$	5599(6)	6139(5)	4806(3)	$H_{17.3'}$	340(4)	935(3)	45(2)
$C_{17'}$	3181(6)	8679(4)	385(3)	H_3	400(3)	457(3)	277(2)
C_3	3891(4)	4621(3)	2199(2)	H_4	372(3)	398(3)	132(2)
C_4	3773(3)	3917(3)	1848(3)	H_7	362(4)	96(3)	278(2)

where A, B and α are the empirical parameters, r_{ij} is the interatomic distances, q_i and q_j are the point charges on atoms, m, n are the kinds of atoms. The A, B and α parameters proposed by A. I. Kitaigorodskii with coworkers[10] were used for calculation purposes. To calculate the hydrogen bond energy, the Morze function was employed:

$$\mu_n(d) = E_0\{1 - \exp[-n(d - d_0)]\}^2 - E_0$$

where E_0 is the hydrogen bond energy for the equilibrium distance d_0, n is the empirical parameter. For the calculation of the electrostatic (Coulomb) interaction used atom charges were obtained through the "Viking" program. When calculating IMIE, the molecules located at not less than 50 Å from the initial one were considered for the sum-

TABLE II (*continuation*)

Anisotropic temperature factors (x 10^4) of non-hydrogen atoms in the MC III molecule. $T_{anis} = \exp -(b_{11}h^2 + b_{22}K^2 + b_{33}l^2 + b_{12}hK + b_{13}hl + b_{23}Kl)$.

Atoms	b_{11}	b_{22}	b_{33}	b_{12}	b_{13}	b_{23}
O_1	105	34	40	−2	−19	−8
O'_1	160	19	27	−2	−21	−11
O_2	120	79	41	−21	−26	−15
O_3	386	40	58	−58	−68	22
O_4	274	76	44	−83	−31	−29
O_5	227	27	65	−23	−68	−10
N'_1	57	28	25	−5	−5	−7
N_2	125	49	44	−45	−25	−7
N_3	111	36	45	4	−33	−15
C'_{22}	48	38	26	−16	−7	−9
C'_3	54	33	29	1	−21	−17
C'_4	90	42	30	−29	−2	13
C'_{4a}	64	27	33	−13	−11	−3
C'_5	84	38	39	−29	−10	20
C'_6	68	37	38	−29	−21	−3
C'_7	63	27	36	−11	−7	−1
C'_{7a}	44	28	27	−1	−2	7
C'_8	80	51	33	7	21	−16
C'_9	66	41	38	−27	−23	−3
C'_{10}	41	27	29	−6	−12	7
C'_{11}	64	60	26	−2	7	−22
C'_{12}	84	66	29	−8	8	−24
C'_{13}	83	61	36	−12	−28	−1
C'_{14}	64	44	40	7	7	−10
C'_{15}	69	36	29	−1	−12	−4
C'_{16}	130	142	37	−18	−70	11
C'_{17}	142	50	51	−30	−42	47
C_3	62	22	34	4	−3	−2
C_4	51	27	38	−3	−5	−9
C_{4a}	51	25	34	2	−1	−4
C_5	71	28	37	−1	−5	−13
C_6	71	18	41	−2	−12	−12
C_7	69	23	38	−4	−8	10
C_8	69	34	29	−2	−13	1
C_{8a}	62	21	38	20	−2	−2

mation region. At such distances the contribution of the more distant electrostatic interactions into the total energy became negligibly small. The total IMIE for all the conjugated interactions with the molecule represents potential energy of the crystalline structure. The calculation was carried out by the program developed at the crystal chemistry laboratory of the Chemical Department of the Moscow State University on a BESM-6 computer.

TABLE III

Coordinates of non-hydrogen (x 10^4) and hydrogen (x 10^3) atoms in the MC IV molecule

Atoms	X	Y	Z	Atoms	X	Y	Z
O_1	2677(4)	1366(2)	2503(36)	$C_{17'}$	8158(3)	1145(2)	2622(20)
O_1	3144(5)	129(2)	2332(0)	C_3	4084(3)	1098(1)	2508(18)
O_2	1424(3)	1555(2)	2540(25)	C_4	3722(3)	783(1)	2583(19)
O_3	562(3)	1189(1)	2658(18)	C_4^a	2937(3)	744(2)	2468(18)
O_4	1962(4)	−234(2)	1824(31)	C_5	2674(4)	388(2)	2578(18)
O_5	1005(5)	−46(2)	2338(23)	C_6	1914(3)	358(2)	2519(21)
$N_{1'}$	5171(2)	1427(1)	2608(15)	C_7	1443(3)	630(2)	2555(18)
N_2	1199(3)	1257(2)	2493(19)	C_8	1708(3)	969(2)	2515(20)
N_3	1625(4)	4(2)	2387(27)	C_{8a}	2461(4)	1042(2)	2550(17)
$C_{22'}$	4856(3)	1110(2)	2516(20)	O_{H2O}	2616(11)	1989(4)	5069(51)
$C_{3'}$	5434(3)	826(1)	2533(17)	$O_{H2O'}$	2885(11)	2460(5)	7018(33)
$C_{4'}$	6837(3)	950(1)	2642(18)	$H_{4'}$	693(3)	67(1)	213(11)
$C_{4a'}$	6113(3)	1051(2)	2576(19)	$H_{6'}$	751(3)	174(1)	233(10)
$C_{5'}$	7348(3)	1218(2)	2484(17)	$H_{7'}$	616(3)	191(1)	274(17)
$C_{6'}$	7139(3)	1565(2)	2581(20)	$H_{8.1'}$	586(4)	37(2)	432(11)
$C_{7'}$	6425(3)	1668(2)	2483(22)	$H_{8.2'}$	484(3)	54(2)	442(12)
$C_{7a'}$	5919(3)	1405(2)	2554(18)	$H_{8.3'}$	587(4)	75(2)	528(11)
$C_{8'}$	5399(7)	590(3)	4350(19)	$H_{9.1'}$	496(4)	41(2)	78(10)
$C_{9'}$	5365(6)	609(3)	742(20)	$H_{9.2'}$	573(4)	47(2)	51(10)
$C_{10'}$	4803(3)	1767(1)	2617(18)	$H_{9.3'}$	519(4)	79(2)	−49(11)
$C_{11'}$	4614(6)	1926(3)	852(20)	$H_{17.1'}$	862(3)	142(2)	213(10)
$C_{12'}$	4358(8)	2233(4)	846(20)	$H_{17.2'}$	847(3)	114(2)	122(11)
$C_{13'}$	4111(4)	2406(2)	2608(28)	$H_{17.3'}$	825(3)	95(2)	320(10)
$C_{14'}$	4213(8)	2262(5)	4195(28)	H_3	371(3)	130(1)	251(19)
$C_{15'}$	4651(6)	1904(3)	4286(16)	H_4	400(3)	52(1)	221(11)
$C_{16'}$	3736(6)	2780(2)	2595(34)	H_7	88(3)	62(1)	278(15)

III. DISCUSSION OF THE RESULTS

1. The structure of the MC molecules

MC I was obtained in ethanol solution upon U.V. irradiation of SP I and subsequently isolated from the solution as dark-purple crystals.[7] The X-ray structure analysis of the SP I initial form and MC I photoproduct formed as a result of a C_{spiro}—O bond photorupture was allowed to follow the characteristic changes in conformation and bond lengths of the SP molecule. A general view of the MC I molecule is given in Figure 1. The photoproduct has an open structure in which O_1 and $C^{22'}_{spiro}$ atoms in a valent bonding with SP I are spaced at 4.17Å. The trans–cis isomer which is H-bonded to a water molecule through a phenolate O_1 atom is present in the crystal ($O_1 \ldots H_{H_2O}$ = 1.77(4)Å,

TABLE III (*Continuation*).

Anisotropic temperature factors (x 10^4) of non-hydrogen atoms in the MC IV molecule.

Atoms	b_{11}	b_{22}	b_{33}	b_{12}	b_{13}	b_{23}
O_1	39	6	628	−4	102	−29
O'_1	44	9	350	−3	55	0
O_2	64	12	761	−3	−77	−36
O_3	39	18	432	1	−11	−51
O_4	71	13	1771	3	−15	−82
O_5	91	19	611	−45	−127	5
N'_1	31	11	217	−1	−38	19
N_2	43	12	335	−2	−69	−42
N_3	48	15	569	−22	−78	52
C'_{22}	30	15	179	−8	−89	−6
C'_3	33	10	196	−2	−14	−15
C'_4	34	11	185	1	69	25
C'_{4a}	30	13	186	2	33	−1
C'_5	30	15	205	−2	79	−29
C'_6	36	15	302	−5	−53	−60
C'_7	36	11	295	−4	1	−19
C'_{7a}	25	11	264	2	−81	50
C'_8	44	13	329	3	44	10
C'_9	35	15	375	0	41	−64
C'_{10}	32	11	295	2	−75	14
C'_{11}	57	12	627	20	−191	−46
C'_{12}	80	16	301	29	−112	−2
C'_{13}	58	14	517	8	−4	54
C'_{14}	63	18	566	25	23	5
C'_{15}	70	16	234	−2	−20	−60
C'_{16}	98	17	863	39	−56	65
C'_{17}	34	17	265	10	127	57
C_3	31	9	207	−4	15	−12
C_4	38	10	229	0	17	−25
C_{4a}	35	14	159	−2	−24	34
C_5	50	11	271	−19	182	7
C_6	40	13	231	−17	−30	62
C_7	40	11	180	−13	−121	20
C_8	35	11	188	0	51	14
C_{8a}	40	12	205	−7	−85	−42
O_{H_2O}	47	24	1558	−14	−110	211

$O_1 \ldots O_{H_2O}$ = 2.75Å [the angle $O_1H_1^{(H_2O)}O(H_2O)$ is 157(5)°]. The molecule slightly deviates from the plane due to the rotation about the C'_{22}—C_3 and C_4—C_{4a} bonds by 11.7° and 4.6°, respectively, which is evidently required by the intramolecular steric conditions or the packing arrangement in the crystal.

The transition to the open form is followed by a full redistribution of the bond lengths in the molecule typical for merocyanate chrom-

TABLE IV

Coordinates of non-hydrogen (x 10^4) and hydrogen (x 10^3) atoms in the MC V molecule

Atoms	X	Y	Z	Atoms	X	Y	Z
O_1	5622(4)	1592(2)	1629(2)	C_6	3167(6)	−558(3)	976(4)
O_2	2469(5)	−2059(3)	1276(4)	C_7	2746(6)	334(3)	569(4)
O_3	1117(6)	−1125(3)	289(5)	C_8	3611(6)	1036(3)	751(3)
O_4	4103(6)	2502(3)	124(4)	C_{8a}	4901(5)	915(3)	1374(4)
O_5	1853(6)	2191(3)	75(4)	C_{10}	7561(6)	−2012(4)	2303(4)
$N_{1'}$	10228(4)	−1480(2)	3189(3)	$H_{N1'}$	1030(5)	−220(3)	314(3)
N_2	2175(6)	−1310(3)	836(4)	$H_{4'}$	1240(5)	114(3)	368(3)
N_3	3165(6)	1976(3)	300(4)	$H_{5'}$	1472(5)	28(3)	424(3)
$C_{22'}$	9181(5)	−790(3)	2915(3)	$H_{6'}$	1510(5)	−151(3)	439(3)
$C_{3'}$	9726(5)	211(3)	3086(3)	$H_{7'}$	1299(5)	−238(3)	390(3)
$C_{4a'}$	11307(5)	−129(3)	3438(3)	$H_{8.1'}$	1054(5)	121(3)	212(3)
$C_{4'}$	12469(6)	391(3)	3694(4)	$H_{8.2'}$	930(5)	158(3)	220(3)
$C_{5'}$	13822(6)	−107(4)	4026(4)	$H_{8.3'}$	1020(5)	36(3)	180(3)
$C_{6'}$	14038(6)	−1109(4)	4110(4)	$H_{9.1'}$	877(5)	25(3)	435(3)
$C_{7'}$	12877(5)	−1655(3)	3863(4)	$H_{9.2'}$	919(5)	127(3)	407(3)
$C_{7a'}$	11560(5)	−1125(3)	3526(3)	$H_{9.3'}$	769(5)	101(3)	382(3)
$C_{8'}$	9678(6)	854(4)	2206(4)	H_4	710(5)	49(3)	225(3)
$C_{9'}$	8787(6)	712(4)	3916(4)	H_5	463(5)	−148(3)	195(3)
C_3	7780(5)	−967(3)	2485(4)	H_7	179(5)	51(3)	5(3)
C_4	6776(5)	−187(3)	2239(3)	$H_{10.1}$	721(5)	−197(3)	160(3)
C_{4a}	5377(5)	−70(3)	1711(3)	$H_{10.2}$	695(5)	−217(3)	293(3)
C_5	4464(5)	780(3)	1526(4)	$H_{10.3}$	852(5)	−240(3)	225(3)

ophore.[11] Here the single bond length in SP I, $N_{1'}$—$C_{22'}$ = 1.453(4)Å, in the MC I structure is reduced to 1.336(6)Å and approaches in its value the C=N double bond length in the five-membered heterocycles, 1.29–1.33 Å.[12] An electrocyclic rupture of the C_{spiro}—O_1 bond leads to a sharp reduction [down to 1.258(7) Å] of the O_1—C_{8a} bond length between the O_1 atom and the benzene fragment in MC I. This value coincides with the length of the zwitterionic bond, for instance, in the DL-serine molecule, 1.26(1) Å.[12] The valence angle $C_{4a}C_{8a}C_8$ [115.4(5)°] in MC I is markedly decreased as compared with the ordinary meaning of 120°, which testifies for the increase of the σ-electronic repulsion from the O_1 atom due to localization of a considerable negative charge on this atom. Such a distribution of bond lengths shows evidence in favour of the bipolar (BP) structure (A) of the MC I molecule (Figure 2). Upon transition from the closed form to the photoproduct, the C_6—N_2 bond length with the p-nitro group N atom reduces from 1.473(5) Å to 1.443(8) Å. In the course of the transition the N_2—O_2 and N_2—O_3 bonds elongate as compared

TABLE IV (*continuation*)

Anisotropic temperature factors (x 10^4) of non-hydrogen atoms in the MC V molecule.

Atoms	b_{11}	b_{22}	b_{33}	b_{12}	b_{13}	b_{23}
O_1	101	20	74	2	−49	−2
O_2	184	47	119	−80	−73	13
O_3	196	79	168	−76	−263	−1
O_4	266	70	113	−140	−129	94
O_5	160	75	144	44	−89	76
N'_1	84	23	26	−15	−14	−6
N_2	126	37	96	−41	−16	11
N_3	144	42	54	5	−46	27
C'_{22}	96	19	29	1	−27	6
C'_3	102	15	35	−33	2	1
C'_{4a}	60	32	18	−19	−20	5
C'_4	106	51	38	−68	−48	−2
C'_5	117	65	33	−53	−22	−7
C'_6	73	49	47	−10	−1	1
C'_7	89	46	43	18	−10	4
C'_{7a}	88	15	27	−24	−27	2
C'_8	130	44	71	−67	−4	60
C'_9	150	42	44	2	−25	−41
C_3	64	27	34	−18	6	−20
C_4	74	30	36	−7	−24	−8
C_{4a}	73	24	26	−15	−13	2
C_5	86	38	32	−32	−12	3
C_6	90	29	47	−11	−17	−12
C_7	101	37	30	−19	−28	−18
C_8	95	24	21	2	−8	7
C_{8a}	63	28	39	18	−9	−5
C_{10}	117	42	67	13	−91	4

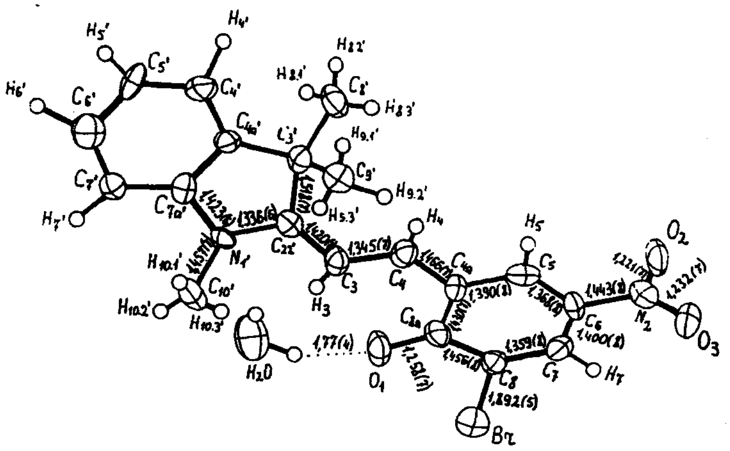

FIGURE 1 A general view, major bond lengths and valence angles of the MC I molecule.

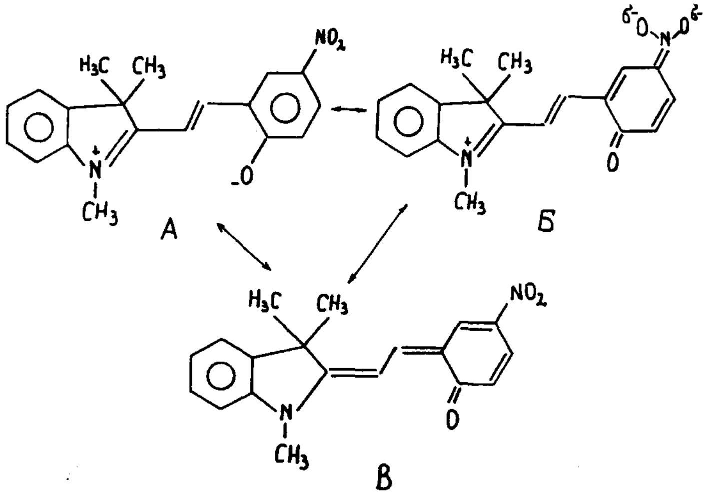

FIGURE 2 Resonance structures giving the main contribution into MC.

with the "equilibrium" value of 126.4° in aromatic nitrocompounds.[13] This points at the strengthening of the S-character of the N_2 atomic orbitals participating in the formation of the C_6—N_2 bond[14] and testifies for the strong resonance interaction of the NO_2 group with the benzene ring. The simultaneous elongation of the C_{4a}—C_{8a} [1.430(8) Å] and C_{8a}—C_8 [1.456(8) Å] bonds as well as the shortening of the C_7—C_8 bond [1.359(8) Å] in the benzene ring points at a considerable contribution made by the resonance quinoid B form into the structure of the p-nitro phenolate fragment (Figure 2).

Attention should be paid also to the shortening of the C_5—C_6 bond [1.368(8) Å] in MC I, which, with the simultaneous shortening of the $C_{22'}$—C_3 bond to 1.420(7) Å as compared with 1.483(5) Å in SP I and even with single C_{sp^2}—C_{sp^2} bond length (1.46 Å)[15] and some elongation of the C_3—C_4 bond [1.345(7) Å] compared to 1.329(6) Å in SP I, indicates a considerable contribution of the resonance quinoid B form into the MC I structure (Figure 2). Mixing structures B and C results in delocalization of the electronic density between the bonds C_{4a}—C_5 and C_5—C_6 and their simultaneous shortening which is thus less evident than for the C_7—C_8 bond. In spite of the fact that the distance O_1 . . . (H_3—C_3) of 2.28(5) Å† is short and the H_3 atom

---

†With the ordinary value of C—H = 1.08 Å this distance is 2.19(5) Å, while when taking into account the average statistical value of C—H = 0.95 Å obtained on X-ray analysis it is 2.24 Å [M. R. Churchill, *Inorg. Chem.*, **12**, 5, p. 1213 (1973)].

must be acidic as follows from the quantum-chemical charge calculations on the MC I atoms (Figure 7), a small torsion rotation about the C_4—C_{4a} bond and an increase of the $C_3C_4C_{4a}$ angle up to 127.4(5)° and the $C_{4a}C_{8a}O_1$ angle up to 125.0(6)° may point at the repulsion between atoms O_1 and H_3. A similar steric repulsion may also take place between atoms H_4 and $C_{3'}$, which may result in increasing the valence angles $C_3C_{22'}C_{3'}$ up to 129.5° and $C_{22'}C_{3'}C_4$ up to 123.9(5)° and a rotation about the $C_{22'}$—C_3 bond by 11.7°.

Thus, the open MC I form is stated to have the most favourable sterically zwitterionic trans–cis A structure with a certain contribution from the B and C structures (Figure 2). Evidently, in MC I crystals the bipolar A structure should be to a considerable extent stabilized due to solvation of the negatively charged phenolate oxygen atom by a water molecule (Figure 1) which thus can markedly affect the electronic structure and stability of the MC molecules.

The crystal structure of MC I solvates allows us to assume that the substitution of the N-methyl group in the indoline ring for the longer and more bulky group may hinder the solvation of the phenolate oxygen atom. For this reason we have undertaken an X-ray study of the MC II N-pentasubstituted whose electronic properties are close to those of the methyl substituent. However, the former must create great steric hindrances for the MC molecule solvation.

Actually, the molecules in the MC II crystals do not form any solvates. Similar to the MC I crystals, the molecules of MC II have a trans–cis structure which is only slightly deviated from the plane due to the torsional rotation about the $C_{22'}$—C_3, C_3—C_4 and C_4—C_{4a} bonds by 5.5, 6.7, and 8.6°, respectively (Figure 3). The indoline fragment is planar, the $C_{8'}$ and $C_{9'}$ atoms go out of the plane by 1.32 and −1.23 Å, respectively. The molecule phenolate ring is slightly distorted, the atoms C_{4a}, C_5 and C_7 deviate from the ring plane by 0.07, 0.07 and −0.09 Å, respectively. The phenolate atom of oxygen O_1 goes out of the ring plane by 0.10 Å.

The bond length distribution in the MC II molecule in general parallels that of the MC I molecule. The absence of water molecules in the MC II crystals solvating the oxygen phenolate atom, however, leads to partial redistribution of electron density. Thus, the O_1—C_{8a} bond length is reduced to 1.228(6) Å, which corresponds to the double C=O bond.[12] The shortening of the O_1—C_{8a} bond in MC II is followed by a subsequent decrease of the valence angle $C_{4a}C_{8a}C_8$ down to 112.8(1)°, which testifies for increasing of the electron repulsion from the O_1 atom. The C_{4a}—C_{8a}, 1.473(6) Å, and C_{8a}—C_8, 1.470(6) Å, bonds become even more elongated, while the C_7—C_8 bond, 1.343(6)

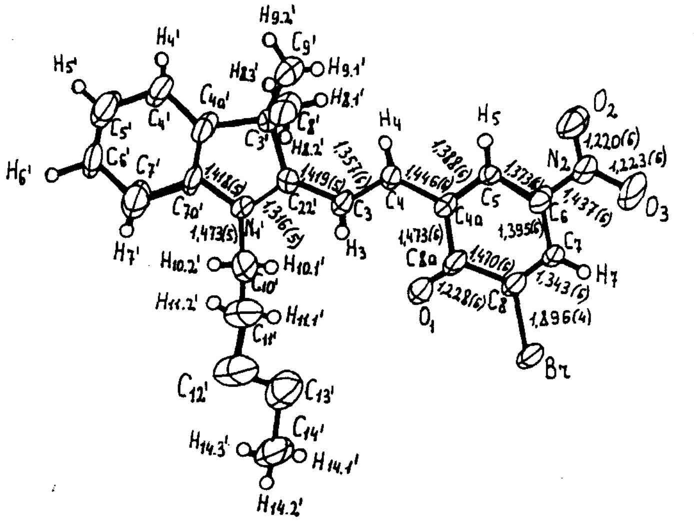

FIGURE 3 A general view, major bond lengths and valence angles of the MC II molecules.

Å, is shortened as compared with the similar bond lengths in MC I. The $O_2N_2O_3$ angle, 121.5(5)°, here is even more than in MC I decreased in comparison with the "equilibrium" value. Such a structure of the p-nitrophenolate fragment indicates an increase in the contribution from the resonance quinoid B form into the zwitterionic A structure of the nonsolvated MC II molecules. The canonic B form contribution is noticed in the structure of the MC II molecules as well as in MC I (Figure 2). The $N_{1'}$—$C_{22'}$ bond, 1.316(5) Å, in MC II is even shorter than in MC I, which speaks in favour of its completely double character and the positive charge localization mainly on the $N_{1'}$ atom.

Therefore, the investigation performed has shown the open SP form structure to be a hybrid structure of resonance A (the largest contribution), B and C forms, while the contribution of each of them, depending on the structure factors in the molecule, may change and the equilibrium shift mostly towards one of them. Hence, the stabilization of open MC molecules must be connected with the stabilization of one of the above resonance structures. The MC I crystal structure testifies for the fact that the solvation of the phenolate O_1 atom stabilizes to a great degree the zwitterionic A structure itself. The stabilization of the canonical B structure can be carried out, for instance, through annelation of some new benzene nuclei to the phenolate benzene ring. This addition of the new benzene nuclei in positions 5–16 and 7–18 should additionally stabilize form B because of preserving the specific aromatic structure of the naphthalene fragment with shortened bonds "*a*" and elongated bonds "*b*", while annelation in positions 6–7 should destabilize it.

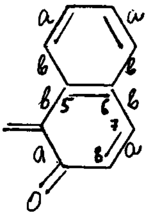

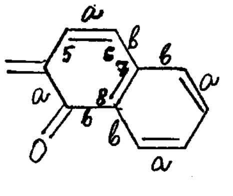

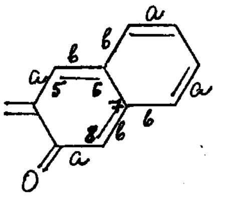

In MC I and II the p-NO_2-substituents in the phenolate ring shift the equilibrium towards the quinoid B form, thus stabilizing the unstable zwitterionic form. On these grounds we assume that the introduction of one more NO_2-group into the o–position to the O_1 atom of this fragment should increase the stability of the open MC form. For this compound it is the MC and not the SP form that is actually more stable in solution.[16] The solutions of this compound are of intense colouring losing their colour upon visible light irradiation.[16] A strong influence of the electron accepting (EA) NO_2-groups accounts for crystallization of dinitro-substituted SP in the coloured MC state. An X-ray study of these crystals has shown the compound to crystallize in two polymorphic modifications: monoclinic and rhombic.

In monoclinic modification—MC III—the molecules have approximately planar trans–cis structure relative to the vinyl $C_3{=}C_4$ bond with slight rotations about the $C_{2'}$—C_3, C_3—C_4 and C_4—C_{4a} bonds by 3.1, 4.7 and 2.7°, respectively, which is analogous to the MC I and II structures. In contrast to MC I and II, however, the oxygen phenolate atom is approximately equivalently disordered in S–cis and S–trans positions to the C_3—C_4 bond. Therefore, the crystal possesses in equal ratios the trans–cis and, for the first time experimentally discovered, trans–trans isomers. The nitro groups are non-coplanar with the benzene plane and form with it angles of 10.3° and 1.6°. The benzene ring itself is planar, the O_1 atom going out of its plane by 0.15 Å and O_1' by 0.01 Å. The N-phenyl substituent turns out of the indoline fragment plane about the $N_{1'}$—$C_{10'}$ bond by 65.1°, which is accounted for by the intramolecular steric conditions, in particular, by repulsion from the H_3 and $H_{7'}$, atoms. The trans–trans isomer in the crystal is solvated by the water molecule ($O_1' \ldots O_{H_2O} = 2.44$ Å) which occupies its position for 50%. As a result of the oriented disarrangement of the phenolate fragment in two positions, the distribution of its bond lengths becomes averaged and no conclusion can be made as for the character of the bond length redistribution upon the introduction of the second NO_2-group into the o–position towards the O_1 atom. Nevertheless, the bond lengths C_6—N_3 = 1.445(7) Å and C_8—N_2 = 1.456(7) Å with both the nitro groups are shortened and the angles $O_2N_2O_3$, 121.3(6)°, and $O_4N_3O_5$, 120.0(6)°, are decreased compared with the "equilibrium" values. This testifies for the strong resonance interaction of these groups with the π-system of the phenolate ring. The C_{4a}—C_5, 1.441(7) Å, and C_{4a}—C_{8a}, 1.432(7) Å, bonds are elongated but the C_6—C_7, 1.368(8) Å, and C_7—C_8, 1.368(7) Å, bonds are shortened in comparison with the normal value in the benzene ring. The remaining bond lengths in the MC III molecule (Figure 4) coincide, within the error limits, with the bond lengths in the MC I and II molecules (Figures 1, 3), although the bond lengths $N_{1'}$—$C_{22'}$, 1.350(6) Å, $C_{22'}$—C_3, 1.439(6) Å, and C_3—C_4, 1.375(6) Å, tend to elongate.

An X-ray study of the rhombic modification—MC IV—has shown the two isomers—trans–cis and trans–trans—to appear in the crystals

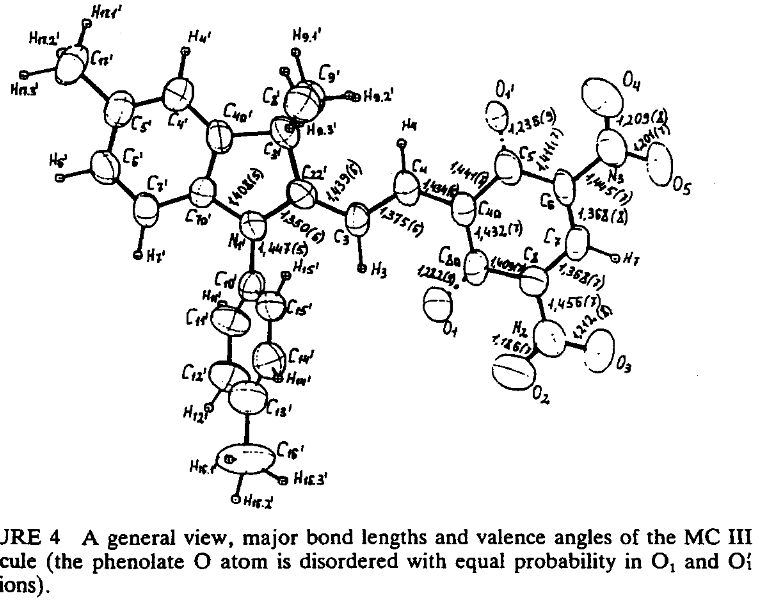

FIGURE 4 A general view, major bond lengths and valence angles of the MC III molecule (the phenolate O atom is disordered with equal probability in O_1 and O_1' positions).

of this compound. The MC IV molecule is nearly planar, the angles of rotation about the $C_{22'}$—C_3 and C_4—C_{4a} bonds being 11.3 and 10.1°, respectively. The nitro groups turn out of the phenolate ring plane by the 13.3 and 6.0° angles. The character of the bond length distribution in MC IV, within the limits of error, coincides with the mode of the bond length distribution in MC III (Figure 5).

As is the case with the MC III crystals, half the molecules of the MC IV crystals are solvated by water molecules (H_2O) and also occupy their positions for 50%. However, in contrast to MC III the solvation in MC IV proceeds not on the O_1 atom of the trans–trans isomer but on the less sterically accessible O_1 atom of the trans–cis isomer [$O_1 \ldots O_{H_2O} = 2.97(3)$ Å], which leads to further turning out of the $N_{1'}$-phenyl substituent from the molecule plane by 87.9°. Such a structure completely excludes the possibility of conjugation of the $N_{1'}$ atom lone electron pair with the phenyl substituent π-system. The energetically unfavourable breaking of the conjugation aroused by steric hindrances during the solvation is evidently compensated by the gain in the MC IV solvation energy. For the non-solvated molecules of the trans–trans MC IV isomer the above structure must be unfavourable. Strong thermal vibrations of the phenyl atoms and their low localization accuracy may point to the statistical disarrangement of the phenyl fragment in several neighbouring po-

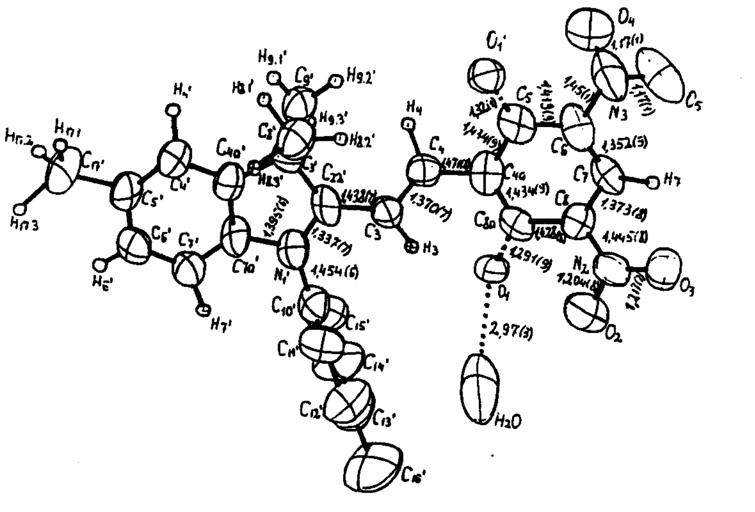

FIGURE 5 A general view, major bond lengths and valence angles of the MC IV molecule (the phenolate O atom is disordered with equal probability in O_1 and O_1' positions).

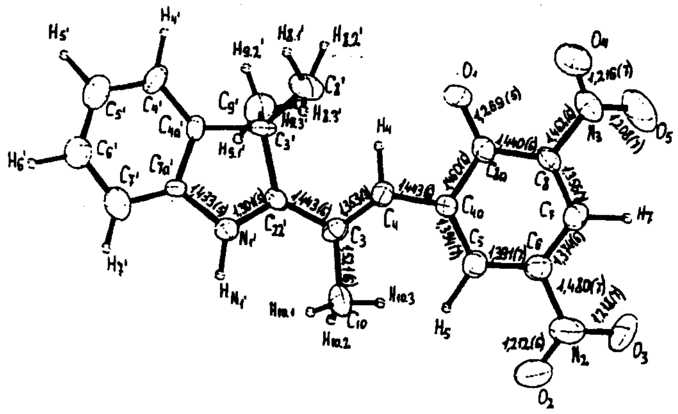

FIGURE 6 A general view, major bond lengths and valence angles of the MC V molecule.

sitions as a result of this fragment becoming more planar in the trans–trans isomer. In the MC IV crystals there are also other water molecules (H_2O) occupying ~25% of their positions at a distance of 2.30(3) Å from the solvated H_2O molecules positions.

Hence, the solvation of the oxygen phenolate atom should be a characteristic feature of the MC molecule in the planar solvents but for the steric hindrances. The introduction of the additional EA NO_2-group into the phenolate fragment stabilizes one more trans–trans isomer which is probably in equilibrium with the trans–cis isomer in solution, which results in their common crystallization.

This conclusion has shown the necessity of a more detailed study of the trans–trans isomer structure. To decide this problem we have carried out an X-ray structure investigation of the o,p-diNO_2-substituted MC V where the vinyl group hydrogen atom is replaced by the CH_3-group, which prevented the formation of the trans–cis isomer. Actually, the MC V crystal molecules have a trans–trans structure (Figure 6) and are chained to each other with the hydrogen bond $O_1 \ldots H'_{N'} = 1.70(4)$ Å which belongs to stable hydrogen bonds.[17] The steric interactions arising between the methyl group C_{10} atoms and the H_5 sin–atom push out the phenolate fragment of the molecule plane due to the rotation about the C_4—C_{4a} bond by 20.3°. However, such a turn may be insufficient to reduce the steric stress in the molecule, while striving to preserve the planar structure with the delocalized electron density interferes with the further acoplanarization of the molecule which leads to the deformation of the valence angles: $C_4C_3C_{10}$ up to 124.6(4)°, $C_3C_4C_{4a}$ and $C_4C_{4a}C_5$ even up to

133.3(4) and 127.0(4)°, respectively. The torsion rotations about the $C_{22'}$—C_3 and C_3—C_4 bonds amount only to 6.1 and 8.3°, respectively.

The absence of disorder in the MC V molecule has allowed us to find out the specificities of the o,p-di-NO_2-substituted MC structure. The o,p-dinitrophenolate fragment is nonplanar. The benzene fragment has conformation "boat" folded along the C_{4a} . . . C_8 line by 7.3° and along C_5 . . . C_7 by 2.3°. The p-NO_2-substituent goes out of the averaged ring plane by 8.3° and the o-NO_2-substituent by 27.2°. The latter is called forth by the steric repulsion of the O_1 and O_4 atoms ($O_1 \ldots O_4$ = 2.734 Å). The bond length O_1—C_{8a} = 1.269(5) Å is close to the length of the same bond in MC I, where the O_1 atom, like that in MC V, participates in a strong hydrogen bond. These bonds are longer than the O_1—C_{8a} bond in MC II where the O_1 atom does not take part in the intermolecular hydrogen interactions. The intramolecular valence angle $C_{4a}C_{8a}C_8$, 115.4(5)°, in MC V is also close to the magnitude of the same angle in MC I proving that the similar σ-electron repulsion from the O_1 atoms exists in both the molecules. It seems strange that in MC V the length of the C_6—N_2 bond with p-NO_2-substituent, 1.480(7) Å, within the limits of error, is the same as the lengths of the analogous bonds in the closed SP^4 and not shortened compared with them, like in MC I, II. The magnitude of the valence angle $O_2N_2O_3$, 125.0(6)°, is close to its "equilibrium" value in aromatic nitrocompounds.[13] All this points at a considerably weaker resonance interaction of the p-NO_2-group with the phenolate fragment π-system as compared with MC I and II. The C_8—N_3 bond, 1.462(6) Å, with the o-NO_2-group is shorter than that with the p-NO_2-group, although it remains longer than in MC I and II. The valence angle $O_4N_3O_5$, 121.6(5)°, also is decreased as compared with the "equilibrium" value. Since it is shown[13] that there is no correlation between the C_{Ac}—N_{NO_2} bond length and the angle of the NO_2-group rotation about this bond, the results obtained confirm a stronger resonance interaction of the o-NO_2-group with the benzene ring π-system as compared with that of the p-NO_2-group. The benzene ring has two bonds which are elongated, those of C_{4a}—C_{8a}, 1.460(6) Å, and C_{8a}—C_8, 1.440(6) Å, and only one bond that is shortened, C_7—C_8, 1.356(7) Å. Taking into consideration the described structure of the o,p-dinitrophenolate fragment, such a distribution of bond lengths in the phenolate ring can hardly be accounted for by the contribution of the quinoid forms B and D and is thought to be more complicated. The quinoid B form contribution into the phenolate fragment structure is also very small, and the elongation of the $C_{22'}$—C_3 bond up to 1.443(6) Å and the further

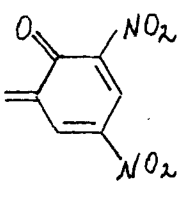

C

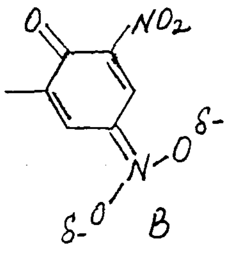

B

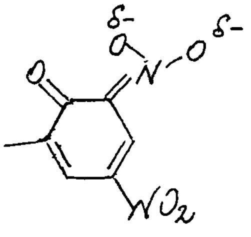

D

shortening of the $N_{1'}$—$C_{22'}$ bond down to 1.301(5) Å as compared with MC I and II points at the reduced contribution of this form into the whole MC V molecule structure. The total distribution of the phenolate fragment bond lengths leads to elongation of the C_{8a}—C_{4a} and C_{8a}—C_8 bonds, which may be the result of the σ-electron repulsion from the negatively charged O_1 atom, and some shortening of the C_6—C_7, 1.374(6) Å, and C_7—C_8, 1.356(7) Å, bonds between the two nitrogroups which may be the result of the electron-acceptor influence of these substituents. The latter conclusion is in accordance with the statistical data,[13] which shows that the bond lengths of the benzene ring attached to the nitrogroup have a tendency to reduce.

It should be noted that in spite of the statistical disarrangement of the o,p-dinitrosubstituted phenolate fragment in MC III and IV, the character of their bond distribution is the same as in MC V.

Thus, the MC molecule with o- and p-NO_2-groups in the phenolate fragment has mainly a bipolar structure (D) with a marked distortion of the phenolate cycle aromaticity.

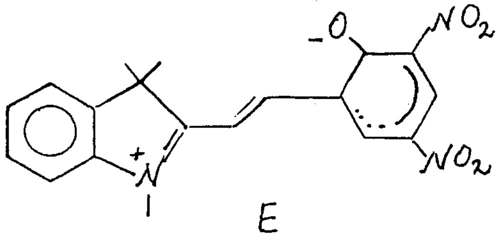

E

An experimentally established fact of the formation of two isomers in the o,p-dinitrosubstituted MC III crystals has put a question of the reasons why these isomers are stabilized and of the possible formation of other MC isomers. In this connection we have paid special attention to the analysis of the MC isomers and their relative stability.

2. Geometrical isomers of the open MC forms

The study of geometrical isomerism and relative stability of the open MC form isomers is extremely important both for the understanding of the SP photochromism mechanism and the explanation of the MC special behaviour, especially, location and appearance of the long-wave absorption which, together with SP photoactivity and MC form stability, is an important factor determining the practical application of the SP systems.[18–20] A large number of theoretical works[21–24] have been devoted to the investigation of the relative stability of monomers

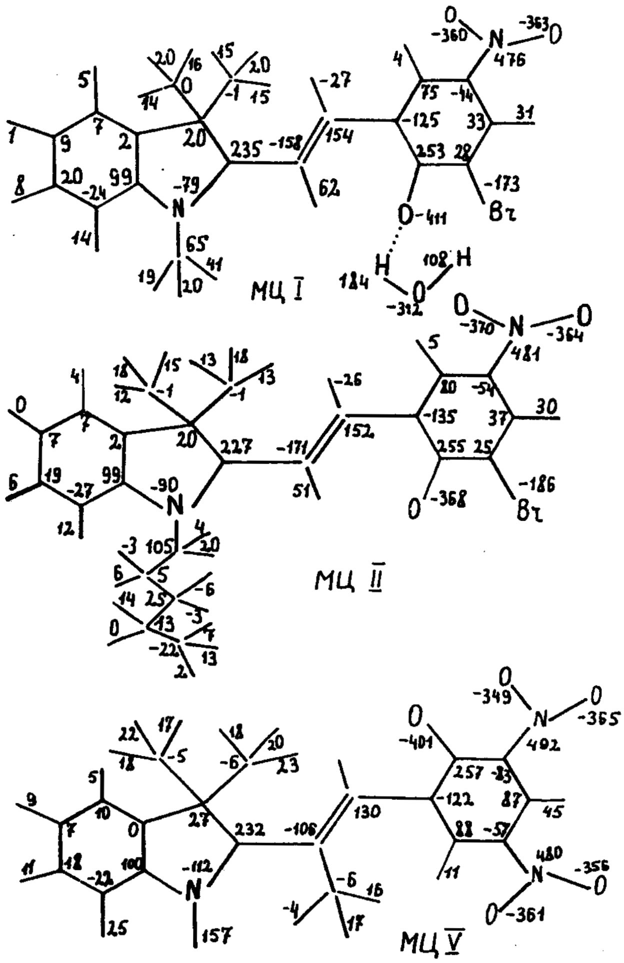

FIGURE 7 Charge distribution (x 10^3) on the atoms of the MC I, II and V molecules obtained using the CNDO/2 method (open bonds correspond to H atoms).

of small model SP and MC and the influence of various substituents on their spectral characteristics. The X-ray analysis of MC I–V has demonstrated the planar MC structure to stabilize due to the electron density delocalization in the molecule. The introduction of the bulky substituents interfering with the planar molecule structure, as is the case with MC V, gives rise to a considerable deformation of the valence angles decreasing the molecule acoplanarization to the utmost. Hence, only planar isomers are stable for sterically unstrained MC molecules. In all the MC crystals investigated there appear trans isomers (E) relative to the vinyl C_3—C_4 bond (Figure 8a,b). The analysis of the MC cis-isomer structure (Figure 8c,d) has shown that strong steric interactions arising in these molecules should interfere with the appearance of the cis isomers. The formation of planar E–S–cis($N_{1'}$, C_4) isomers relative to the $C_{22'}$—C_3 bond (Figure 8e,f) is also impossible because of steric conditions. This is confirmed by the structure of compound VI in which the steric interactions actually interfere with the appearance of the E–S–cis (N_1, N_2) planar structure and lead to the formation of a less favourable E–S–trans (N_1, N_2) isomer with the N_2 and O centres brought nearer. Therefore, the final formation of only planar trans–cis and trans–trans isomers

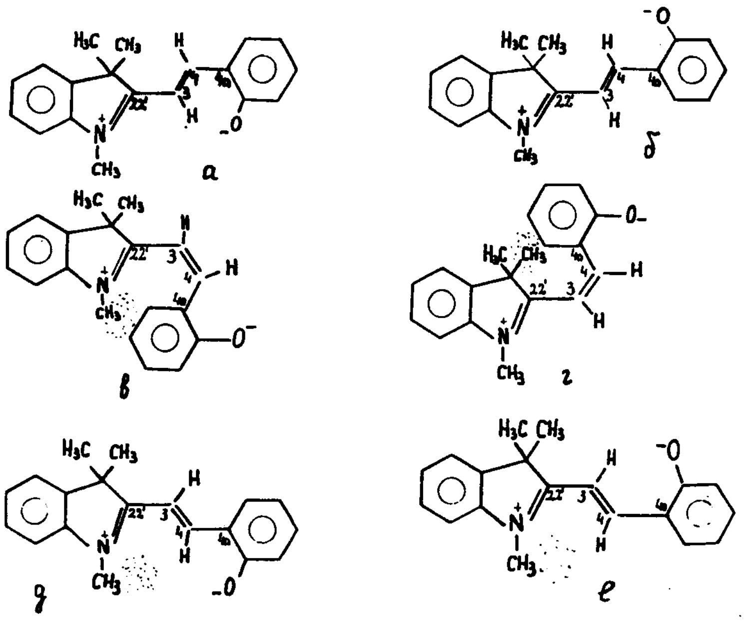

FIGURE 8 Geometrical isomers of planar MC molecules.

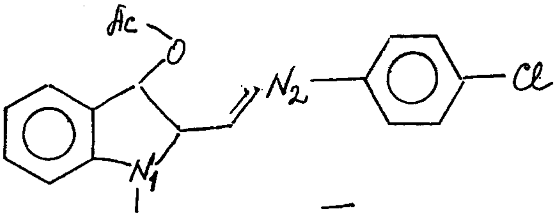

VI

as the main equilibrium products is mostly probable for sterically nonstrained MC in solutions (Figure 8a,b). The first of the isomers appears in all the MC I–IV crystals as well as in the open form of benzothiozolic SP-(TMC) studied,[25] while the second of them only in the MC III-IV crystals whose molecules have two nitrosubstituents in the phenolate fragment. In this connection there arises a question of the relative instability of these two isomers and the reasons of stabilization of the trans–trans isomers upon the introduction of a second nitrogroup into the o-position of the phenolate fragment. Besides, to better understand the SP photochemistry structural mechanism it was important to establish which of the two isomers is the first to form on the reaction coordinate. We have used quantum-chemical methods CNDO/2 and INDO to try qualitatively evaluate the relative energetic stability of these isomers and the transition barrier between them. For the purposes of calculations we have used the MC II geometry obtained upon the X-ray analysis, which contained one nitrogroup in the p-position to the oxygen atom of the phenolate fragment, and the MC V geometry containing two nitrogroups in the o- and p-positions of this fragment. To create similar steric conditions in these MC V molecules the methyl group at a C_3 atom was replaced by a hydrogen atom and the valence angles $C_3C_4C_{4a}$ and $H_3C_3C_4$ were assigned the standard meanings of 120°. Bond lengths and valence angles in the calculation process were not optimized,

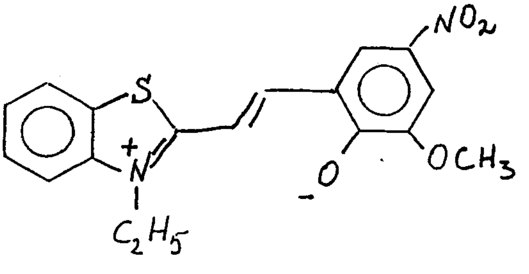

ТМЦ

since the current semi-empiric quantum-chemical methods reproduce poorly the complex resonance BP structures similar to those discovered in the investigated MC. Figure 9a illustrates the dependence of the MC II molecules relative energy on the angle of the C_4—C_{4a} bond for every 20°. The energy of the trans–cis isomer was assumed to be zero. As is clear from the diagram, the energy of the transition from the trans–cis to the trans–trans isomer obtained in both the methods is approximately the same and is as high as ~20 kcal/mol in the CNDO/2 method and ~24 kcal/mole in the INDO method. Here the trans–cis isomer has appeared to be just slightly more favourable than the trans–trans one (with the first method by ~1 kcal/mole, and the second one by ~4.5 kcal/mole). The dipole moment of the isomers obtained in both the methods is the same and amounts to ~17 D.

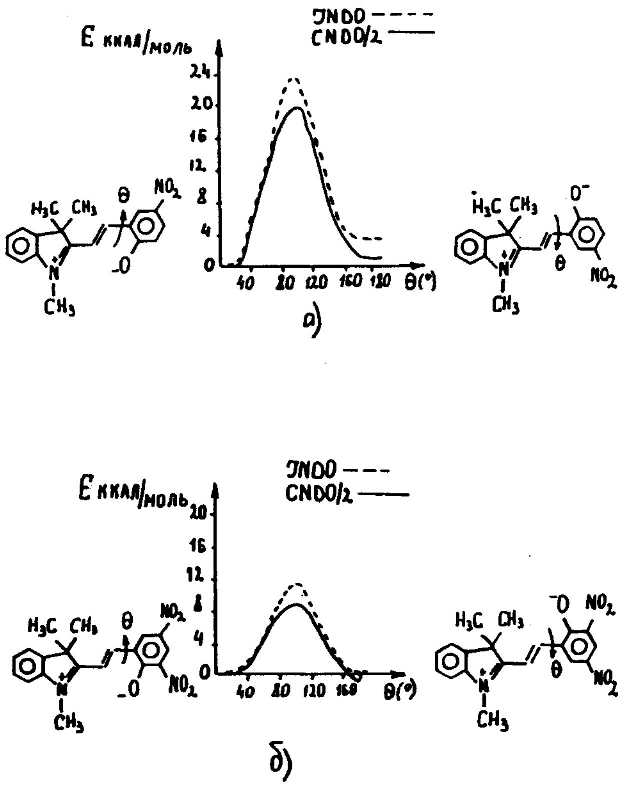

FIGURE 9 The dependence of the relative energy of MC molecules with one NO_2-group (a) and two NO_2-groups (b) in the phenolate fragment on the rotation angle O. The energy of the trans–cis isomer is assumed to be zero.

Figure 9b shows the dependence of the relative energy of the model molecule with two nitrogroups in the phenolate ring on θ. Calculations using both the CNDO/2 and INDO methods testify for a double decrease of the barrier of trans–cis → trans–trans isomerization (for the first method up to ~9 kcal/mole, for the second up to ~12 kcal/mole). For the CNDO/2 method the trans–trans isomer even becomes ~2 kcal/mole more favourable than the trans–cis isomer. The dipole moments of the dinitrosubstituted MC isomers are approximately the same and are as high as 20 D. The energies of the rotational barrier obtained without optimization in the framework of semiempirical methods are obviously too high to be overestimated. Thus, in the analogous semiempirical estimation of salicylidenanilines molecules[26] the barrier of the phenyl ring rotation about the single bond in the conjugated system appeared to be one and a half times higher compared with the "ab initio" calculations of the analogous model systems, although qualitatively the results of these calculations coincided. The polar MC molecule solvation in solution may also affect the relative stability of these isomers and the transition barrier value between them. A short-wave shift of the MC absorption spectrum maximum with an increase of solvent polarity[16] points at the fact that in the ground state such high-polar molecules interact violently with solvent polar molecules. For both the methods the dipole moment of MC acoplanarization increases to ~22 D in nitrosubstituted MC and to ~23 D in dinitrosubstituted MC with an angle of rotation about the C_4—C_{4a} bond equal to 90°. That is why in polar solvents a more polar non-planar molecule must be more solvated than a planar one which is an additional factor stabilizing the transient state and reducing the transition barrier between the planar isomers. Due to the fact that the planar isomers studied have very close dipole moments, the solvation of these molecules should not change the general character of energetic correlation between them. Based on the results obtained it may be concluded that the trans–cis and trans–trans MC isomers are close in their energies. For MC with one nitrogroup in the phenolate fragment between them there is a marked transition barrier, while the introduction of two nitrosubstituents into the o- and p-positions reduces this barrier so that in solution these isomers can easily transform one into another. Really, the cocrystallization of both the isomers of the o,p-dinitrosubstituted MC III and IV also testify for the fact that the packing energy of these isomers is practically the same and they are present in the solution in approximately the same concentrations. Based on the X-ray analysis of MC V it is believed that the reduction of the barrier of rotation about the C_4—C_{4a} bond upon the introduction of two EA nitrogroups into the phenolate fragment may be connected with the increased contribution of the D form into the molecule structure, which decreases the $\pi-\pi$-interaction energy of this fragment with the rest of the molecule. The appearance of the trans–cis isomer in MC I and II with one NO_2-group in the phenolate fragment which were obtained in a photochemical way from the closed SP form indicates that this isomer is preceding the energetically equivalent trans–trans isomer on the reaction coordinate of the open MC form formation from the closed SP. It is also the main final produce for MC without EA substituents or with one nitrogroup in the phenolate fragment, and in MC with two EA nitrosubstituents it is in equilibrium with the trans–trans isomer.

The data obtained give rise to doubt as for the existing point of view that the complex character of the absorption spectrum of the SP open forms is associated with the presence of four various stereoisomers in solid phase and in solution.[27,28] More to that, the calculations of the absorption spectra of the 2H-chromen model valence isomers show that these isomers are undiscernible in the long-wave absorption region.[21] The papers[29–32] have suggested an idea of the association of coloured and coulourless SP forms to explain the MC spectral characteristics. The similarity of the MC absorption spectra in nonpolar solvents at low temperatures, in the amorphous state and in thin crystalline homogeneous films testifies for the fact that the coloured SP form in liquid and solid phases possesses the same structure. In this connection a considerable attention should be paid to the MC molecule packing and the intermolecular interaction energy in crystals.

3. The character of molecule packing and the energy of intermolecular interactions in MC crystals

It has appeared that the crystals of all the MC investigated have different packing modes. In the MC II crystals the molecules are packed in centrosymmetric stacks by a "head-to-tail" mode I″, I, I′, I‴ and so on along the "b" axis (Figure 10). For clarity purposes the molecules in the figures are presented as arrows directed from the indoline cationic molecule fragment to the phenolate anionic molecule fragment coinciding with the long molecule axis, i.e., with its dipole moment vector. The plane of the molecule is perpendicular to that of the figure. In such stacks the neighbouring molecules overlap and are parallel and oriented opposite to each other. Molecules

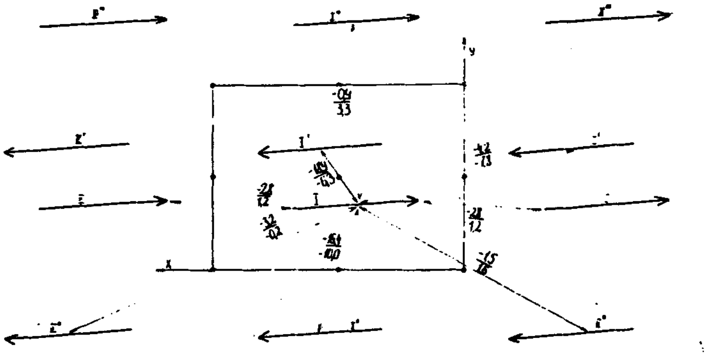

FIGURE 10 Packing arrangement of the MC II molecules in stacks. (An arrow coincides with the long axis of the molecule; the plane of the molecule is perpendicular to the plane of the figure).

I, I′ are most closely located in the stacks. The shortest intermolecular contact of 3.21 Å appears between the O_1 oxygen atom of the anion part of one molecule and the $N_{1'}$ nitrogen atom of the cationic part of another one. Table V lists the shortest intermolecular contacts in stacks between the I and I′, I″ molecules. Such a stacking arrangement makes us believe that between molecules exist both the strong Van der Waals and electrostatic interactions. With the aim of quantitative evaluation of the contributions from these interactions we have performed the estimation of the MC II crystal structure energy. Figure 10 shows the values (in kcal/mole) of the Van der Waals energy (numerator) and the electrostatic intermolecular energy (denominator) in and between the stacks obtained in the framework of the atom–atom "6-exp"-potentials scheme taking into consideration the electrostatic interactions. Since the intermolecular interactions energy obtained by this method depends considerably on the chosen parameters of potentials and the magnitude of atomic charges, the same parameters were used for all the crystals and the same method (CNDO/2) with similar parameters was used to learn the atomic charges. The energy of intermolecular interactions in stacks is approximately an order of magnitude higher than the energy of the near-neighbour molecular interactions in various stacks. The energy of electrostatic interactions, which in organic crystals usually constitutes only an inconsiderable part of the Van der Waals energy, in the MC II crystals reaches almost half the energy of the Van der Waals interaction. The total interaction energy between the nearest-neighbouring molecules I and I in the stacks and the more remote I and I″ molecules appears

TABLE V

The main shortest intermolecular contacts (Å) between molecules I, I′ (d_1) and I, I″ (d_2) in the MC II stacks

Type of contact	d_1	d_2
$Br \ldots C_{7a}$	3.89	
$O_1 \ldots N_{1'}$	3.21	
$O_1 \ldots C_{8'}$		3.60
$O_1 \ldots C_{22'}$	3.43	
$O_1 \ldots C_{10'}$	3.27	
$N_{1'} \ldots O_1$	3.21	
$C_{22'} \ldots O_1$	3.43	
$C_{7a'} \ldots Br$	3.89	
$C_{7'} \ldots N_2$		3.84
$C_{7'} \ldots C_6$		3.73
$C_{7'} \ldots C_7$		3.76
$C_{6'} \ldots C_7$		3.70
$C_{4a} \ldots C_{10'}$	3.55	
$C_5 \ldots C_{11'}$		3.47
$C_{8'} \ldots O_1$		3.60
$C_{8a} \ldots C_{10'}$	3.34	
$C_{10'} \ldots O_1$	3.27	
$C_{10'} \ldots C_{4a}$	3.55	
$C_{10'} \ldots C_{8a}$	3.34	
$C_{11'} \ldots C_5$		3.47

to be almost the same and amounts to 25 and 26 kcal/mole, while between the stacks is in the range of −5.5 ± +2.5 kcal/mole. The only exclusion is an interstack interaction of the I and II′ molecules: −4.2/−7.8 kcal/mole (for convenience purposes the molecules in different stacks have different numeration). Such a clearly expressed anisotropy of intermolecular interaction in the MC II crystals accounted for by an anomalously high interaction energy in the stacks allows us to assume the "head-to-tail" associates to be energetically stable enough to exist in solution too.

The total energy (Van der Waals' and electrostatic) of the MC II crystal structure is −50.7 kcal/mole, −35.3 kcal/mole of it constituting the Van der Waals interaction energy, and −15.4 kcal/mole—the electrostatic energy. The TMC crystals[25] have an analogous packing arrangement. The shortest contacts, 3.391 and 3.488 Å, discovered in their associates are those between the N_1 and C'_{22} atoms of one molecule and the phenolate ring plane of another.

The MC I crystals have a different crystal structure. The solvation of the anionic part of the MC molecules does not allow the "head-to-tail" arrangement as in the MC II associates in which the anionic part of the molecule is located over the cationic part of another. The

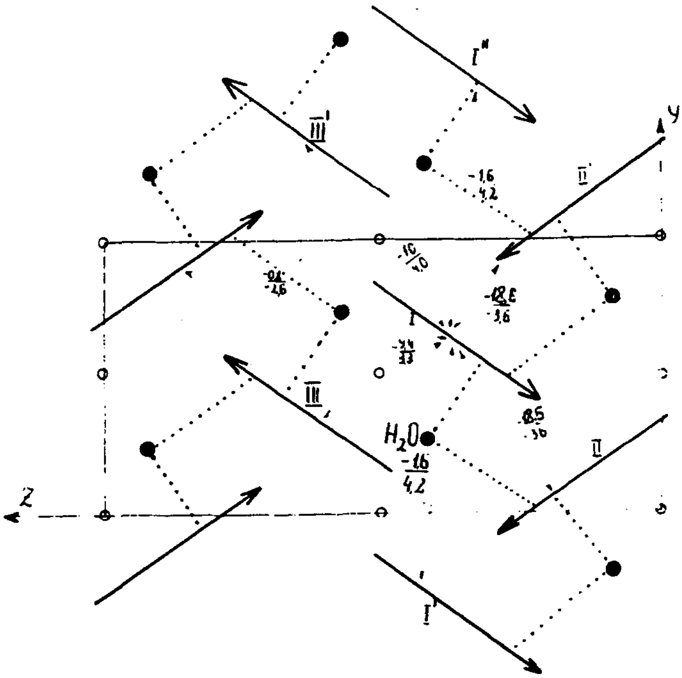

FIGURE 11 Packing arrangement of the MC I molecules in layers.

water molecules of the MC I crystals bind the MC molecules with hydrogen bonds in bands with flaky packing: I', II, I, II', I'' etc. (Figure 11). One of these hydrogen bonds with the O_1 atom being stronger ($O_1 \ldots O_{H_2O} = 2.75$ Å, $O_1 \ldots H_{H_2O} = 1.77$ Å), it forms a stable solvate I · H_2O, while another being a weaker one—a bond with the O_2 atom of the near-neighbour molecule II nitrogroup ($O_2 \ldots O_{H_2O} = 3.12$ Å). The main shortest intermolecular contacts in the layers are given in Table VI.

The energy estimation of the MC I crystal structure shows (Figure 11) that the interaction between the I and II molecules hydrogen bound with water molecules is the strongest intermolecular interaction in the structure. Taking into account the energy of these hydrogen bonds† (I . . . $H_2O = -5.5$ kcal/mole, H_2O . . . II = 1.8 kcal/mole), the energy of interaction between the molecules in the associate

---

†The energy of the hydrogen bond O . . . H—O was determined using the Morze potential and the recommendation from Ref. 17.

TABLE VI

The main shortest intermolecular contacts (Å) between molecules I, II (d_1), I, II′ (d_2) and I, III (d_3) in the MC I layers

Type of contact	d_1	d_2	d_3
$O_1 \ldots N_2$	3.62		
$O_2 \ldots C_3$		3.41	
$O_3 \ldots C_4$	3.64		
$O_3 \ldots C_3$	3.60		
$O_3 \ldots C_{9'}$	3.39		
$N_2 \ldots O_1$		3.62	
$N_2 \ldots C_3$		3.43	
$N_2 \ldots C_4$		3.52	
$C_3 \ldots O_2$	3.41		
$C_3 \ldots N_2$	3.43		
$C_3 \ldots O_3$		3.60	
$C_4 \ldots N_2$	3.52		
$C_4 \ldots C_6$	3.54		
$C_4 \ldots O_3$		3.64	
$C_{4a} \ldots C_6$	3.50		
$C_{4a} \ldots C_7$	3.49		
$C_{4a} \ldots C_5$		3.61	
$C_6 \ldots C_{4a}$		3.50	
$C_6 \ldots C_{8a}$	3.51		
$C_5 \ldots C_{4a}$	3.61		
$C_6 \ldots C_4$		3.54	
$C_7 \ldots C_{4a}$		3.49	
$C_7 \ldots C_{8a}$	3.44		
$C_7 \ldots C_8$		3.66	
$C_8 \ldots C_7$	3.66		
$C_8 \ldots C_8$	3.65	3.55	
$C_{8a} \ldots C_6$		3.51	
$C_{8a} \ldots C_7$		3.44	
$C_{7'} \ldots C_{7a'}$			3.68
$C_{7'} \ldots C_{7'}$			3.66
$C_{7a'} \ldots C_{6'}$			3.66
$C_{7a'} \ldots C_{7'}$			3.66
$C_{10'} \ldots O_{H2O}$			3.39

$I \cdot H_2O \ldots II$ reaches −18.6/−3.6 kcal/mole. The total energy of the MC I crystal structure, −51.4 kcal.mole, is close to the analogous value for the MC V crystals. The Van der Waals component of the energy is equal to −43.4 kcal/mole, and the electrostatical one is −8.1 kcal/mole.

The MC I and II packing modes described above are thought to be typical for solvated and unsolvated MC molecules. The crystal structures of MC III and IV serve as a confirmation of this conclusion. It is only the trans–trans isomer that is solvated in the MC III crystal (i.e. half the molecules) and the crystal structure of this compound

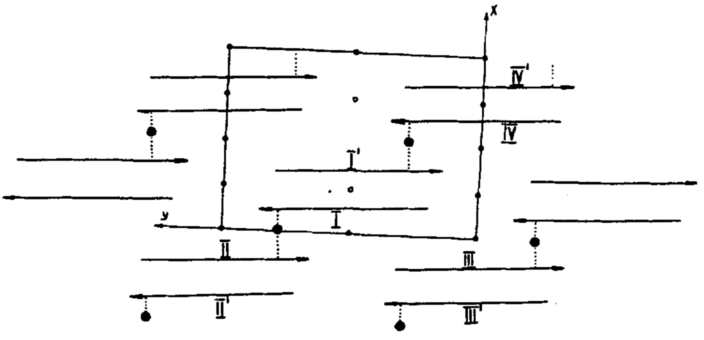

FIGURE 12 Packing arrangement of the MC III molecules in layers.

comprises the features typical for MC I and MC II packings. This structure is schematically represented in Figure 12. The MC III crystal structure consists of centrosymmetric dimeric associates I, I′ of the "head-to-tail" type as in the MC II crystals. Water molecules bind the dimeric associates by hydrogen bonds. The shortest intermolecular contacts for the MC III molecules are given in Table VII.

Only the trans–cis isomer molecules are solvated in the MC IV crystals, i.e. also only half the molecules. However, in the MC IV crystals, in contrast to the MC III ones, the "head-to-tail" associates are not formed (Figure 13). Obviously the solvation of the sterically less accessible O_1 atom of the trans–trans isomer in the MC IV creates bigger steric hindrances in the formation of such associates than the solvation of the trans–cis isomeric peripheral O_1 atom in MC III. As in the MC I crystals, the water molecules of the MC IV crystals bind the MC IV molecules "head-to-head" by hydrogen bonds. Table VIII lists the major shortest intermolecular contacts in the layers. Unfortunately, to estimate unambiguously the intermolecular interaction energy in the associates of various isomers and between them in the MC III and IV crystals is impossible because of the orientation disorder of the molecules.

The molecules in the MC crystals are bound with each other along the "y" axis by the chains of stable hydrogen bonds existing between the H_1 atom of the indoline fragment of one molecule and the phenolate O_1 atom of another (N_1—H_1 . . . O_1 = 1.70 Å). The layers formed in the crystal packing of the chains are perpendicular to the chain direction and parallel to the XOZ plane (Figure 14). The MC V crystal layers consist of friable translational stacks I′, I, I″ along the "a" axis which permeate into one another with their anionic and

TABLE VII

The main shortest intermolecular contacts (Å) between molecules I, I′ (d_1), I, II (d_2) and I, III (d_3) in the MC III layers

Type of contact	d_1	d_2	d_3
$O_1 \dots C_{9'}$	3.34		
$O_1 \dots O_2$		3.57	
$O_1 \dots O_3$		3.08	
$O_1 \dots N_2$		2.99	
$O_1 \dots C_7$		3.41	
$O_1 \dots C_8$		3.05	
$O_2 \dots C_{4'}$	3.19		
$O_2 \dots C_{5'}$	3.36		
$O_2 \dots O_2$		3.15	
$O_2 \dots N_2$		3.47	
$O_3 \dots C_{5'}$	3.53		
$O_3 \dots C_{17'}$	3.44		
$O_3 \dots O_1$		3.08	
$O_3 \dots C_{14'}$		3.21	
$N_2 \dots C_{4'}$	3.58		
$N_2 \dots C_{5'}$	3.33		
$N_2 \dots O_1$		2.99	
$N_2 \dots O_2$		3.47	
$C_{4'} \dots O_2$	3.19		
$C_{4'} \dots N_2$	3.58		
$C_{5'} \dots O_2$	3.36		
$C_{5'} \dots N_2$	3.33		
$C_{7'} \dots C_{7'}$			3.37
$C_{9'} \dots O_1$	3.34		
$C_8 \dots O_1$		3.05	
$C_8 \dots C_{8a}$		3.30	
$C_{8a} \dots C_8$		3.30	
$C_{8a} \dots C_{8a}$		3.39	
$C_{14'} \dots O_3$		3.21	
$C_{17'} \dots O_3$	3.44		

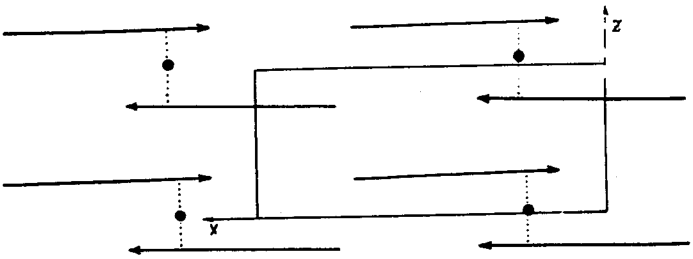

FIGURE 13 Packing arrangement of the MC IV molecules in layers.

TABLE VIII

The main shortest intermolecular contacts (Å) between molecules I, I′ (d), I, I″ (d_2), I, II′ (d_3), I, II″ (d_4) in the MC IV layers

Type of contact	d_1	d_2	d_3	d_4
$O_{1'} \ldots C_6$	3.48			
$O_{1'} \ldots O_4$		3.44		
$O_{1'} \ldots N_3$	3.52			
$O_4 \ldots O_{1'}$	3.44			
$O_3 \ldots C_{22'}$		3.50		
$O_3 \ldots C_{11'}$		3.59		
$O_3 \ldots C_3$		3.48		
$O_2 \ldots C_{15'}$	3.31			
$O_2 \ldots C_{11'}$		3.33		
$N_3 \ldots O_{1'}$		3.52		
$N_2 \ldots C_3$	3.58			
$N_2 \ldots C_3$		3.60		
$C_{22'} \ldots O_3$	3.50			
$C_{4'} \ldots C_{17'}$			3.59	
$C_{4'} \ldots C_{17'}$				3.57
$C_{5'} \ldots C_{5'}$			3.55	
$C_{5'} \ldots C_{17'}$			3.55	
$C_{5'} \ldots C_{5'}$				3.55
$C_{11'} \ldots O_3$	3.59			
$C_{11'} \ldots O_2$	3.33			
$C_{15'} \ldots O_2$		3.31		
$C_{15'} \ldots O_3$		3.61		
$C_{17'} \ldots C_{5'}$				3.55
$C_3 \ldots O_3$	3.48			
$C_4 \ldots C_7$	3.58			
$C_4 \ldots C_8$		3.62		
$C_{4a} \ldots C_8$	3.63			
$C_5 \ldots C_6$	3.63			
$C_5 \ldots C_5$	3.56			
$C_5 \ldots C_6$		3.55		
$C_5 \ldots C_5$		3.56		
$C_6 \ldots O_{1'}$		3.48		
$C_6 \ldots C_5$	3.55			
$C_6 \ldots C_5$		3.63		
$C_7 \ldots C_4$	3.55			
$C_7 \ldots C_4$		3.58		
$C_7 \ldots C_{4a}$		3.66		
$C_8 \ldots C_4$	3.62			
$C_8 \ldots C_{4a}$		3.63		
$C_{8a} \ldots C_{8a}$	3.51			
$C_{22'} \ldots O_3$	3.50			

cationic parts. The anionic parts of the neighbouring stacks form centrosymmetric dimeric associates I, II of the "head-to-head" type, the cationic parts of the neighbouring stacks forming centrosymmetric dimeric associates I, III of the "tail-to-tail" type. The main shortest intermolecular contacts in the layers are listed in Table IX.

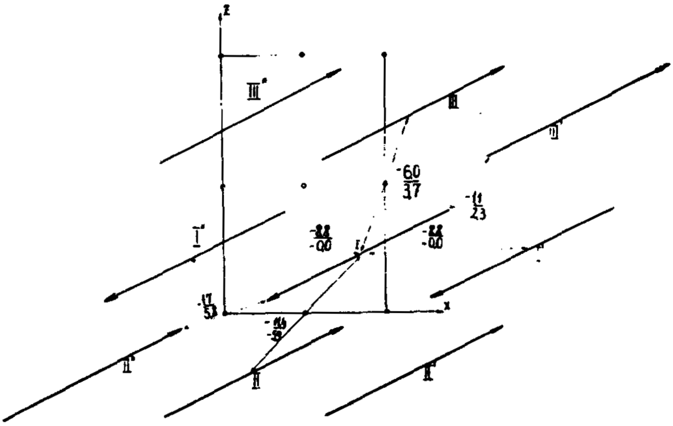

FIGURE 14 Packing arrangement of the MC V molecules in layers.

The energy calculations for the MC V crystal structure show (Figure 14) that the strongest intermolecular interactions are those between the hydrogen bonded molecules in the chain, −8.2/−9.2 kcal/mole, and those in the "head-to-head" centro-symmetric I, II associates in the layer, −11.4/−5.9 kcal/mole.

The total energy of the MC V crystal structure is −54.5 kcal/mole (the Van der Waals component is −36.5 and electrostatic one is −18.0 kcal/mole) being close to the energies of the MC I and II crystal structures. However, the ratios of the Van der Waals and electrostatic energies components in the MC I, II, V crystal structures are different. In the crystal structures of MC II and V, where the molecules in stacks and layers are arranged plane-to-plane to one another, the electrostatic energy component of the crystal structure reaches 30 and 33%, respectively, and plays a significant role in crystal formation. In the MC I crystal, where the hydrogen-bonded solvated molecules are arranged in a flaky packing mode, the electrostatic component of the crystal structure energy lowers down to 15%, though remaining higher than in most organic crystals.

The crystal data obtained just for a few open MC forms of SP demonstrate a pronounced tendency of MC to form various associates in a crystal. The reason for that is planar structure and high polarity of MC molecules, since, besides the Van der Waals interaction, the electrostatic and dipole–dipole interactions also play important roles in associate formation. The energy calculations of the MC crystal structures show that the electrostatic interaction in the associates may reach 50% of the Van der Waals interaction. The most stable asso-

TABLE IX

The main shortest intermolecular contacts (Å) between molecules I, I′ (d_1), I, II (d_2), I, II″ (d_3), I, III (d_4) in the MC V layers

Type of contact	d_1	d_2	d_3	d_4
$O_4 \ldots C_5$		3.46		
$O_5 \ldots C_{10}$		3.40		
$O_5 \ldots O_3$			3.26	
$O_2 \ldots N_{1'}$	3.39			
$O_2 \ldots C_{7a'}$	3.49			
$O_3 \ldots O_5$			3.26	
$O_5 \ldots O_5$			3.56	
$N_3 \ldots C_5$		3.59		
$C_{5'} \ldots C_4$	3.64			
$C_{5'} \ldots C_{4a}$	3.56			
$C_{5'} \ldots C_5$	3.68			
$C_{5'} \ldots C_{5'}$				3.50
$C_{6'} \ldots C_{9'}$				3.75
$C_{7'} \ldots C_{9'}$				3.64
$C_{7a'} \ldots C_{9'}$				3.67
$C_{8'} \ldots C_7$	3.58			
$C_{9'} \ldots C_{7'}$				3.64
$C_{9'} \ldots C_{7a'}$				3.67
$C_4 \ldots C_{5'}$	3.64			
$C_{10} \ldots C_5$		3.40		
$C_{4a} \ldots C_{5'}$	3.56			
$C_{4a} \ldots C_7$		3.62		
$C_5 \ldots C_{5'}$	3.68			
$C_5 \ldots O_4$		3.46		
$C_5 \ldots N_3$		3.59		
$C_5 \ldots C_8$		3.64		
$C_7 \ldots C_8$	3.58			
$C_7 \ldots C_{4a}$		3.62		
$C_8 \ldots C_5$		3.64		
$N_{1'} \ldots O_2$	3.39			

ciates are formed in the MC II crystals in which the molecules are packed "head-to-tail" in stacks one over another. The total energy of the Van der Waals and electrostatic interactions, even if to exclude the dipole–dipole interaction in these stacks, is ≈26 kcal/mole. In the MC crystals the associates form hydrogen-bonded solvated MC molecules. Hence, the energy of electrostatic attraction between them decreases and the total energy of the Van der Waals and electrostatic interactions is −22 kcal/mole. The most stable associates in the MC V crystals (17 kcal/mole) form hydrogen-bonded molecules in chains and molecules I, II arranged plane-to-plane and "head-to-head" in the layers.

The formation of sufficiently stable associates in the MC I–V crystals with diverse packing modes allows us to assume that these associates may last in solution as well. Usually only the most stable energetically and favourable for packing molecule association modes are found out in crystals, so the diversity of these modes can be even greater in MC solutions. Thus, in non-polar solvents, the "head-to-tail" associates formation will be mostly probable for the MC molecules which are not bonded by an intermolecular interaction with the solvent molecules. In proton polar solvents the formation of solvates giving various hydrogen-bonded associates will be mostly probable. Based on the X-ray data we may conclude that N_1'-alkyl substituents hinder the MC trans–cis isomer solvation, however, not preventing the "head-to-tail" associates formation. The N_1'-methyl substituent does not hinder the trans–cis isomer solvation by water molecules. The solvated molecules of the MC trans–cis isomers form associates due to hydrogen bonds with the solvate molecules. The substituents at the N_1' atom do not prevent the trans–trans isomer solvation. The solvated MC trans–trans isomer can form both the "head-to-tail" associates and those at the expense of the solvate molecules. The N_1'-phenyl substituent does not prevent the "head-to-tail" associate formation but creates greater steric hindrances in the trans–cis isomer formation than the N-methyl substituent does. The solvation of the N-phenyl substituted MC leads to the energetically unfavourable turning out of the N-phenyl substituent of the molecule plane by 90°. The solvate and associate formation is an additional factor stabilizing the high polar MC forms and is considered to be a more probable reason for appearance of the complicated MC absorption spectrum than the assumption of the diverse MC isomers existence.

The discovered[29–32] spontaneous processes of ordering the coloured form upon irradiation of the SP solutions in aliphatic solvents may be also connected with the associate formation. The result of these processes is the formation of globules of submicron sizes composed of crystal-like nuclei with an amorphous coat and displaying unusual optical and electrical properties.[33–37]

The data obtained allow us also to consider the most probable structural mechanism of photoconversions in SP.

4. The most probable structural mechanism of SP photoconversions

There is yet no common point of view on the problem of the detailed mechanism of SP photochemical reactions. The most important problem is identification of the intermediate isomer responsible for induced absorption in the region of 440 nm. Recently several highly probable energetic ways of forming the coloured B form from the colourless SP A have been suggested.[38-40]

Based on the molecular and crystal data on the initial SP and obtained from them MC forms, one can suggest the most probable structural mechanism of photochromic conversion of the initial SP (Figure 15) into the final product. As was shown earlier[4] and has been already mentioned in the Introduction, the SP photochemical characteristics (Figure 15a) are mainly conditioned by the fact that already in the ground state the C_{spiro}—O bond split in photoexcitation is elongated and weakened owing to the specific $n - \sigma^*$ orbital interactions which become even more intensive in the transition to

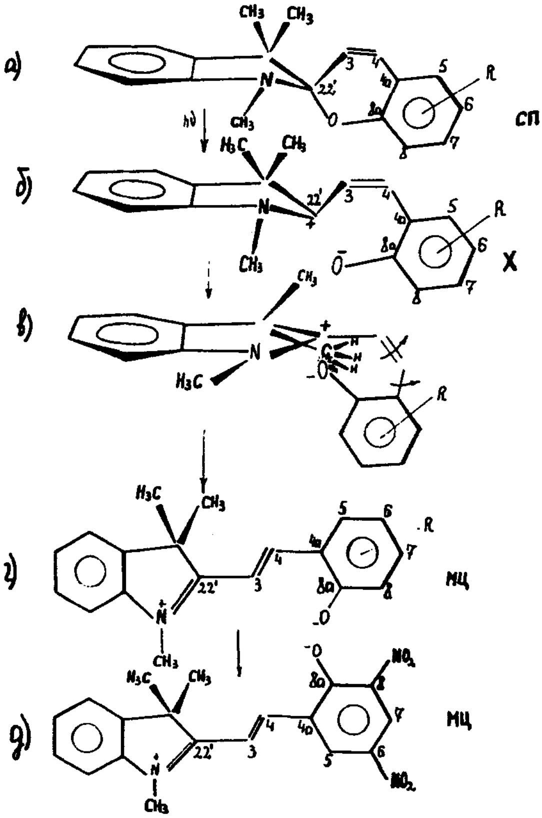

FIGURE 15 The most probable structural mechanism of photo- and thermochromic conversions of spiropyrans based on the X-ray data on SP and MC structure.

the excited state to result in the heterolytic bond dissociation. In the produced X-isomer the pyramidal configuration of the C_{spiro} carbocation (Figure 15b) is extremely unstable and fast changing into the more stable planar configuration (Figure 15c). The non-valent distances estimations show the distances between the C_{spiro} and O atoms in such a model structure to increase up to ~2.1 Å and those between the phenolate fragment atom and the spin-methyl group reduce down to ~1.8–2.1 Å. Such a structure should give rise to strong steric repulsions between the phenolate fragment and methyl group atoms. The reduction of steric interactions may be connected with the rotation of the phenolate fragment about the C_3—C_4 bond to lead further to the formation of a planar trans–cis isomer (Figure 15d) with a conjugated π-bond system. The structure of this isomer is confirmed by an X-ray analysis. In the MC molecules including EA nitro substituents in the phenolate fragment the transition barrier between the trans–cis (Figure 15d) and trans–trans (Figure 15e) isomers decreases, both the isomers being in solution in equilibrium. The formation of other planar isomers, as was mentioned in Chapter 2, has proved to be unfavourable from the point of view of steric hindrances. In non-polar solvents, in the process of reaction various associates of MC and SP molecules are formed stabilizing the bipolar MC structure and conditioning the unusual spectral, electrical and optical properties of their solutions. In polar solvents the determining role belongs to solvation of SP and, especially, MC molecules by polar solvent molecules which additionally stabilize the MC bipolar structure and prevent the formation of associates.

In spirothiopyrans (STP), unlike spiropyrans, the elongation of the C_{spiro}—S bond is accounted for by steric interactions[41] and not by specific orbital interactions. Based on the data on the photochemical properties and structure of the investigated STP we have assumed the C_{spiro}—S bond rupture in these compounds to occur in a homolytic way by the vibration mechanism. The C_{spiro}-radical pyramidal configuration produced in the bond rupture in STP, as is shown for other systems,[41] is more stable than the planar one due to σ-superstress. Hence, neither packing of the C_{spiro} atom pyramidal configuration, nor further isomerization of the molecules evidently occur. And the obtained coloured form in STP, unlike that in SP, is not a zwitterionic trans–cis structure but merely its intermediate thermodynamically unstable X isomer[42]:

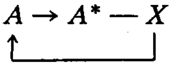

IV. CONCLUSIONS

1. The open MC form of spiropyrans is shown to have a zwitterionic A structure with some contribution from the canonical B form. The structural factors stabilizing these forms are found out.

2. The EA substituents are established to stabilize the MC form due to localization of the O atom negative charge and formation of quinoid B structure. The MC molecules solvation stabilizes the zwitterionic A structure. Annelation of additional benzene nuclei to the phenolate ring in the 5–6 and 7–8 positions should stabilize the MC structure due to the stabilization of the canonical B form and should destabilize it on the annelation in positions 6–7.

3. For sterically unstressed MC molecules in crystals and solutions the main final products are represented by planar trans–trans and trans–cis isomers of almost similar energies. Here the trans–cis isomer precedes the trans–trans one on the reaction coordinate. In MC with one nitrogroup in the o- or p-positions of the phenolate fragment between the isomers there is a marked energetical transition barrier, hence a prevailing content of trans–cis isomers in solution and the presence of only this isomer in the crystals. The introduction of two nitrogroups in the o- and p-position of this fragment reduces considerably the transition barrier; in solution these isomers can easily turn one into another, forming cocrystals in crystallization.

4. Even the crystal structure data on a small number of open MC forms of SP testify for the pronounced tendency of MC to form diverse associates in crystals. Crystal-structure energy calculations show that, besides the Van der Waals interactions, the electrostatic and dipole–dipole interactions also play a significant role in the formation of such associates and stacks. The most stable associates are formed on the crystallization of non-polar aproton solvents and have a "head-to-tail" structure being packed in centrosymmetric stacks. In polar solvents the solvent molecules form stable solvates with MC molecules which prevent the formation of such associates. The solvated MC molecules give various associates due to stable hydrogen bonds of the "head-to-head" and "head-to-head, tail-to-tail" types. The bulky N1́-alkyl substituents hinder the solvation of the MC trans–cis isomer, however, not preventing the "head-to-tail" associate formation. The N1́-methyl substituent does not hinder the trans–cis isomer solvation by water molecules. The solvated molecules of the trans–cis MC isomers do not form any "head-to-tail" associates giving associates due to hydrogen bonds with the solvate molecules. The substituents at the N1́ atom do not prevent the trans–trans isomer sol-

vation. The solvated trans–trans MC isomers can form both the "head-to-tail" associates and those which are hydrogen-bonded with the solvate molecules. The N$_1'$-phenyl substituents do not prevent the "head-to-tail" associate formation, however, creating greater steric hindrances in the trans–cis isomer solvation than the N-methyl substituent does. The N-phenyl substituted MC solvation leads to the unfavourable energetically turning out of the phenyl substituent of the molecule plane by 90°. The formation of stable solvates and associates is an additional factor stabilizing the MC form not only in crystals but in solution as well.

5. Based on the molecular and crystal structure data of the initial SP and MC forms produced from them the most probable structural mechanism of photochromic SP conversion is suggested.

References

1. V. A. Barachevskii, G. I. Lashkov and V. A. Tsekhomskii, "Photochromism and its Applications" (in Russian), 280 pp., Khimiya, Moscow (1977).
2. "Organic Photochromes" (in Russian), Ed. A. V. El'tsov, 288 pp. Khimiya, Leningrad, (1982).
3. S. M. Aldoshin and L. O. Atovmyan, "Problems of Crystal Chemistry" (in Russian), Nauka, Moscow (1984).
4. S. M. Aldoshin and L. O. Atovmyan, *Izv. Akad. Nauk SSSR* (ser. khim.) No. 9, pp. 2009–2015 (1985).
5. V. N. Andrianov, Z.Sh. Safina and B. L. Tarnopolskii, Roentgen-75, Automated system of programs for crystal deciphering, Chernogolovka (1975).
6. A. N. Chekhlov, *Kristallographiya*, **26**, 596 (1981).
7. S. M. Aldoshin, L. O. Atovmyan, O. A. Dyachenko and M. M. Galbertshtam, *Izv. Akad. Nauk SSSR* (ser. khim.), **2720**, (1981).
8. S. M. Aldoshin and L. O. Atovmyan, *Izv. Akad. Nauk SSSR*, (ser. khim.) No. 9, pp. 2016–2023 (1985).
9. "Quantum-chemical Methods of Molecule Calculations" (in Russian), Ed. Ya.A. Ustyunyuk, Khimiya, Moscow, 256 pp. (1980).
10. T. V. Timofeeva, Chernikova N. Yu, and P. M. Zorkii, Uspekhi khimii, XLIX **966** (1980); **966**; Mirskaya, K. V., Kozlova, I. E. and Bereznitskaya, V. F. *Phys. Stat. Sol.*, **62**, p. 291 (1974).
11. S. Dahne, *Science*, **199**, 1163 (1978).
12. "Molecular Structures and Dimensions." Oosthoek's Uitgevers mij Utrecht, The Netherlands, v. A1 (1972).
13. J. R. Holden and C. Dickinson, *J. Phys. Chem.*, **81**, 1505 (1977) .
14. D. Williams, *J. Amer. Chem. Soc.*, **89**, 4280 (1967).
15. H. A. Bent, *Chem. Revs.*, **61**, 275 (1961).
16. K. G. Japaridze, *Spirochromenes* (in Russian), Metsniereba, Tbilisi, p. 112 (1979).
17. L. N. Kuleshov, Thesis, Moscow, p. 190 (1982).
18. R. C. Bertelson, In "Photochromism," Chapt. III, Ed. G. H. Brown, J. Wiley Intersci., New York, p. 45–432 (1971).
19. E. Fischer, *Fortschr. Chem. Forsch.*, **7**, 605 (1967) .
20. V. P. Barachevskii, *Zh. Vsesoyuzn. Khimich. Obshch. im.* D. I. Mendeleeva, **19**, 423 (1974).

21. V. I. Minkin, B. Ya. Simkin, L. E. Nivorozhkin and B. S. Lukyanov, *Khimiya geterotsikl. soedinenii*, No. 1, 65 (1974).
22. B. Ya. Simkin, V. I. Minkin and L. E. Nivorozhkin, *Khimiya geterotsikl. soedinenii*, No. 9, 1180 (1978).
23. B. Ya. Simkin and V. I. Minkin, *Khimiya geterotsikl. soedinenii*, No. 2, 177 (1980).
24. B. Ya. Simkin, S. P. Makarov and V. I. Minkin, *Khimiya geterotsikl. soedinenii*, No. 8, 1028 (1982).
25. E. Miller-Srenger and Guglielmetti, R., *Acta Crystallogr.*, **B38**, 1980 (1982).
26. S. M. Aldoshin and L. O. Atovmyan, *Khim. fizika*, **3**, 915 (1984).
27. T. Bercovici, R. Heiligman-Rim and E. Fischer, *Mol. Photochem.*, **1**, 23 (1969).
28. C. Balny, R. Donzon, T. Bercovici and E. Fischer, *Mol. Photochem.*, **1**, 225 (1969).
29. A. A. Parshutkin and V. A. Krongauz, *Mol. Photochem.*, **6**, 437 (1974).
30. V. Krongauz, J. Kiwi and M. Gratzel, *J. Photochem.*, **13**, 89 (1980).
31. V. D. Arsenov, A. A. Parshutkin, V. S. Marevtsev and M. I. Cherkashin, *Izv. Akad. Nauk SSSR* (ser. khim.) No. 9, 1976–1983, 1987–1993 (1984).
32. V. D. Arsenov, V. S. Marevtsev and M. I Cherkashin, *Izv. Akad. Nauk SSSR* (ser. khim.) No. 9, 1984–1986 (1984).
33. V. A. Krongauz and E. S. Goldburt, *Nature*, **271**, 43–45 (1978).
34. V. A. Krongauz, S. N. Fishman and E. S. Goldburt, *J. Phys. Chem.*, **82**, 2469–2474 (1978).
35. G. R. Meredith, V. A. Krongauz and D. J. Williams, *Chem. Phys. Letters*, **87**, 289–294 (1982).
36. G. R. Meredith, D. J. Williams, S. N. Fishman, E. S. Goldburt and V. A. Krongauz, *J. Phys. Chem.*, **87**, 1697–1701 (1983).
37. D. J. Williams, *Angew. Chem. Intern.*, 23/9, 690–703 (1984).
38. S. A. Krysanov, M. V. Alfimov, *Chem. Phys. Letters*, **91**, 77–80 (1982).
39. Y. Kalisky and D. J. Williams, *Chem. Phys. Letters*, **86**, 100–104 (1982).
40. Y. Kalisky, T. E. Orlowski and D. J. Williams, *J. Phys. Chem.*, **87**, 5333–5338 (1983).
41. S. M. Aldoshin, A. S. Kholmanskii and L. O. Atovmyan, *Izv. Akad. Nauk SSSR* (ser khim.) No. 3, 576–582 (1986).
42. M. J. S. Dewar, *J. Amer. Chem. Soc.*, **106**, 669–682 (1984).